

Theory of central peak and acoustic anomaly in cubic BaTiO₃ close to ferroelectric transition

Akira Onuki*

Department of Physics, Kyoto University, Kyoto 606-8502, Japan

(Dated: March 9, 2026)

Abstract

We present a Ginzburg-Landau theory on statics and dynamics of BaTiO₃-type ferroelectrics in the paraelectric phase with the cubic structure, where the order parameter is the polarization \mathbf{p} . Unique effects are caused by the electrostrictive (ES) coupling between \mathbf{p} and the elastic displacement \mathbf{u} . We show that the ES coupling gives rise to a central peak in the Fourier-Laplace transform of the displacement time-correlation function at small wave numbers. It emerges and grows with a narrow width as the transition is approached. Such central peaks have long been observed in a number of scattering experiments in various ferroelectrics, but their origin has not been well understood. From the acoustic part of the displacement dynamic correlation we obtain the frequency-dependent elastic moduli $C_{11}^*(\omega)$, $C_{12}^*(\omega)$, and $C_{44}^*(\omega)$, whose singular parts arise from the ES coupling. We then calculate the singular sound velocity and attenuation. In the central peak and the elastic moduli, the frequency ω appears in the scaled form $\omega\tau_D$, where τ_D is the Debye relaxation time in the frequency-dependent dielectric constant.

Keywords: ferroelectric transition, central peak, acoustic anomaly, electrostrictive coupling

* e-mail: onuki@scphys.kyoto-u.ac.jp (corresponding author)

1. Introduction

Ferroelectric transitions have been studied extensively in theories and experiments [1–8], where the static dielectric constant ϵ grows as $(T - T_0)^{-1}$ obeying the Curie-Weiss law in the paraelectric phase as a function of the temperature T . Many such systems including barium titanate BaTiO_3 undergo weakly first-order transitions with structure changes [9–12], where the transition temperature T_c is slightly above the pseudocritical temperature T_0 . In the ordered phase with $T < T_c$, spontaneous polarization appears resulting in domain formation. To understand the transition behavior, use has been made of the Landau theory [5, 13–19], where the free energy of the polarization density \mathbf{p} is a polynomial of \mathbf{p} with the gradient term and the electric energy added. As a unique feature, the electric field \mathbf{E} consists of the contribution from the electrode charges and that from the interior dipoles, where the latter largely cancels the former and gives rise to the dipole-dipole interaction. In particular, Kretschmer and Binder [19] accounted for this depolarization effect in their Landau free energy to calculate the polarization profile in film samples.

The ferroelectric transitions are strongly influenced by the solid elasticity, where \mathbf{p} and the elastic strains $e_{\alpha\beta}$ ($\alpha, \beta = x, y, z$) are coupled in the free energy [1, 2, 6]. The coupling is of the bilinear form $\sum_{\alpha, \beta, \gamma} d_{\alpha\beta\gamma} p_\alpha e_{\beta\gamma}$ in piezoelectric systems, where $d_{\alpha\beta\gamma}$ are constants. A famous example is uniaxial KH_2PO_4 (KDP), where the elastic modulus C_{66} tends to 0 and becomes dependent on the frequency ω on approaching the transition in the paraelectric phase [20–23]. Such strong elastic anomaly can be explained by the Landau-Khalatnikov theory [24] with the long-range dipolar interaction included [25, 26]. On the other hand, in systems with a centrosymmetric crystal structure, the coupling is electrostrictive (ES) in the paraelectric phase, where it is of the third order form $\sum_{\alpha, \beta, \gamma, \nu} d_{\alpha\beta\gamma\nu} p_\alpha p_\beta e_{\gamma\nu}$ in the lowest order with $d_{\alpha\beta\gamma\nu}$ being constants [27–34]. This coupling becomes piezoelectric with appearance of nonvanishing average polarization. Famous examples are BaTiO_3 and uniaxial triglycine sulfate (TGS) [3], whose crystal structures are cubic and monoclinic, respectively, in paraelectric states. Theories on the near-critical sound absorption were presented for BaTiO_3 [35, 36] and TGS [37, 38] many years ago. The acoustic anomaly in electrostrictive systems [39–41] are much smaller in magnitudes than that in piezoelectric systems.

In various ferroelectrics, central peaks have been observed in the dynamical scattering amplitudes [23, 42–57], which emerge and grow with a narrow width as $T \rightarrow T_c$ both in piezoelectric and electrostrictive systems. In strontium titanate SrTiO_3 , however, the

central peak was observed for the zone-boundary $(1/2, 1/2, 3/2)$ wave vector near the 105 K antiferrodistortive, second-order phase transition, where the order parameter is the staggered rotation angles of the oxygen octahedra but the polarization fluctuations are also enhanced with $\epsilon \sim 10^3$. Previously, the origin of the central peaks was ascribed to the thermal entropy diffusion (Rayleigh scattering) [23, 49, 57], to impurities [58], and to droplets or small domains [59]. In light scattering, the dielectric tensor at optical frequencies depends on the polarization and/or the strains [23, 51, 60–62], which can result in the central peaks.

From our viewpoint, the central peaks are produced by slowly relaxing components in the stress tensor, which can arise from the piezoelectric or electrostrictive (ES) coupling without impurities, vacancies, and small domains. We gain this picture from our calculation of the time-correlation of \mathbf{u} at small wave vector \mathbf{q} with the ES coupling for BaTiO₃. We shall see that its temporal Fourier transform has a narrow peak centered at $\omega = 0$, which exhibits the characteristic feature of the central peak of BaTiO₃ [43, 53, 54]. Thus, it should constitute an essential part of the central peak in the neutron and light scattering amplitudes [63]. We note that the longitudinal acoustic modes exhibit critical anomaly in BaTiO₃. In this calculation we also obtain the frequency-dependent elastic moduli $C_{ij}^*(\omega)$, where $C_{11}^*(\omega)$ and $C_{12}^*(\omega)$ exhibit significant critical anomaly but $C_{44}^*(\omega)$ is nearly nonsingular [41].

The organization of this paper is as follows. In Sec.II, the statics in the Landau theory will be discussed. In Sec.III, the equal-time polarization correlations will be calculated. In Sec.IV, we will calculate the time-correlations of the polarization and displacement fluctuations, where the frequency-dependent elastic moduli and the central peak will be derived.

2. Statics

2.1. Free energy of \mathbf{p} and \mathbf{u}

We consider a BaTiO₃-type cubic system slightly above the transition without free charges. The polarization \mathbf{p} exhibits critical fluctuations. The sample is confined in a $L \times L \times H$ cell with metal electrodes at $z = 0$ and H . Here, $d \ll H \ll L$, where d is the lattice constant. The sample volume is $V = L^2H$. We write the Maxwell electric field as $\mathbf{E}(\mathbf{r}) = -\nabla\Phi(\mathbf{r})$ with $\mathbf{E} = \mathbf{0}$ in the electrodes, where the potential Φ arises from the electrode charges and the interior dipoles. The electric induction is $\mathbf{D} = \mathbf{E} + 4\pi\mathbf{p}$ with $\nabla \cdot \mathbf{D} = 0$ in the sample. In this geometry, the net surface charges at $z = 0$ and $z = H$ are written as Q_0 and $-Q_0$, respectively, while the potential at $z = 0$ and $z = H$ can be set equal to Φ_a and 0,

respectively [64–68].

The free energy functional for \mathbf{p} and the elastic displacement \mathbf{u} is given by

$$\mathcal{F}(\{\mathbf{p}\}, \{\mathbf{u}\}) = \int d\mathbf{r} \left[\frac{1}{8\pi} |\mathbf{E}|^2 + f_B + f_{el} + f_{int} + f_T \right], \quad (1)$$

where $\int d\mathbf{r}(\dots)$ is the sample integration and $\int d\mathbf{r} |\mathbf{E}|^2/8\pi$ is the electric energy [4, 64–68]. To see how the electric energy is related to \mathbf{p} , let us superimpose small changes, $\delta\mathbf{p}$, $\delta\mathbf{E}$, and δQ_0 on \mathbf{p} , \mathbf{E} , and Q_0 , respectively. The incremental change in the electric energy becomes

$$\int d\mathbf{r} \mathbf{E} \cdot \delta\mathbf{E}/4\pi = \Phi_a \delta Q_0 - \int d\mathbf{r} \mathbf{E} \cdot \delta\mathbf{p}, \quad (2)$$

where the first term vanishes at fixed Q_0 or at $\Phi_a = 0$. Thus, we assume either of these two conditions. Then, the functional derivative of the electric energy with respect to \mathbf{p} is simply given by $-\mathbf{E}$. In this paper, we omit the surface free energy in Eq.(1) [19] and the effect of the surface layers [68] will be discussed briefly in the last paragraphs in Secs.2.4 and 4.1.

The appropriate free energy at a fixed Φ_a is given by the Legendre transform $\tilde{\mathcal{F}} = \mathcal{F} - \Phi_a Q_0 = \mathcal{F} - \int d\mathbf{r} \mathbf{E} \cdot \mathbf{D}/4\pi$ [4, 67, 68], which leads to $(\delta\tilde{\mathcal{F}}/\delta\mathbf{p})_{\Phi_a, \mathbf{u}} = (\delta\mathcal{F}/\delta\mathbf{p})_{Q_0, \mathbf{u}}$ (see Eq.(19)). In $\tilde{\mathcal{F}}$, the electric energy density is given by $-|\mathbf{E}|^2/8\pi - \mathbf{p} \cdot \mathbf{E}$, which gives rise to the one-dimensional free energy in the Kretchmer-Binder theory (see their Eq.(12)) [19].

2.2. Bulk free energy of \mathbf{p} and first-order ferroelectric transition

In Eq.(1), f_B is the bulk free energy density of \mathbf{p} , where one of the easy axes is along the z axis. Up to the sixth order terms it is written as [1, 2, 15–17, 30–32]

$$f_B = \frac{1}{2} A |\mathbf{p}|^2 + \alpha_{11}^0 \sum_{\alpha} p_{\alpha}^4 + \alpha_{12}^0 (p_x^2 p_y^2 + p_y^2 p_z^2 + p_z^2 p_x^2) + \sum_{\alpha, \beta, \gamma} \alpha_{\alpha\beta\gamma}^0 p_{\alpha}^2 p_{\beta}^2 p_{\gamma}^2 + \frac{1}{2} C |\nabla \mathbf{p}|^2, \quad (3)$$

where α_{11}^0 , α_{12}^0 , and $\alpha_{\alpha\beta\gamma}^0$ are constants. Hereafter, the Greek indices refer to the Cartesian coordinates, x , y , and z . The coefficient A is related to the temperature T as

$$A = a_1 (T/T_0 - 1). \quad (4)$$

For a weakly first-order transition, T_0 is the pseudocritical temperature slightly below the first-order transition temperature T_c . For BaTiO₃, the fourth order terms are small and the sixth order terms are indispensable in describing the phase behavior. See Appendix A, where the fourth-order terms produced by the ES interaction will be calculated.

As Eqs.(2) and (3) indicate, the dielectric susceptibility χ and the dielectric constant $\epsilon = 1 + 4\pi\chi$ in the linear regime are related to A as

$$\chi = 1/A, \quad \epsilon = 1 + 4\pi/A \cong (4\pi/a_1)/(T/T_0 - 1), \quad (5)$$

which is the Curie-Weiss law for $0 < A \ll 1$. The surface effect on the dielectric constant will be discussed in the last paragraph in Sec.2.4.

At low ambient pressures, BaTiO₃ undergoes a weakly first-order ferroelectric transition with a cubic-to-tetragonal structure change at $T_c \cong 400\text{K}$. The transition becomes second-order with increasing the pressure ($\gtrsim 35 \text{ Kbar} = 3.5\text{GPa}$) [9–11]. This can be explained by the pressure-dependence of the coefficients in the Landau model. In particular, the experimental values of a_1 , T_0 , and T_c at low pressures depend on the experimental groups. We mention two examples:

$$a_1 = 1.8 \times 10^{-2}, \quad T_0 = 384 \text{ K}, \quad T_c - T_0 = 17 \text{ K}, \quad (6a)$$

$$a_1 = 3.6 \times 10^{-2}, \quad T_0 = 388 \text{ K}, \quad T_c - T_0 = 10 \text{ K}, \quad (6b)$$

where we use the data by Kashida *et al.* [40] in Eq.(6a) and those by Li *et al.* [31] in Eq.(6b). Here, $a_1 \ll 1$, whose implication was discussed by Ginzburg [13]. The a_1 in Eq.(6b) is twice larger than that in Eq.(6a), but both give $\epsilon \sim 1.5 \times 10^4$ and $A \sim 10^{-3}$ at $T = T_c$, which are the maximum of ϵ and the minimum of A , respectively, in equilibrium paraelectric BaTiO₃. It is worth noting that $a_1 = 1.24$ for TGS [3] and $a_1 = 0.41$ for KDP [21].

In the gradient free energy we set $|\nabla \mathbf{p}|^2 = \sum_{\alpha,\beta} (\nabla_\alpha p_\beta)^2$, where ∇_α is the α -th component of $\nabla = \partial/\partial \mathbf{r}$. This form of the gradient free energy much simplifies the calculations to follow, though it can be anisotropic generally (see Appendix B) [15–17, 31, 32]. From Eq.(3) we find the growing mean-field correlation length given by

$$\xi = (C/A)^{1/2} = \xi_0(T/T_c - 1)^{-1/2}, \quad \xi_0 = (C/a_1)^{1/2}. \quad (7)$$

where $\xi_0 \sim 10\sqrt{C}$ from Eq.(6). In Eq.(50) below, we will have $\sqrt{C} \cong 1.5 \text{ \AA}$ for BaTiO₃. Thus, we find $\xi_0 \sim 10 \text{ \AA}$, which is longer than the lattice constant $d = 4 \text{ \AA}$.

2.3. Elastic, electrostrictive, and thermoelastic free energies

The f_{el} in Eq.(1) is the elastic free energy of cubic solids written as

$$f_{\text{el}} = \frac{1}{2} \sum_{\alpha,\beta} \sigma_{\alpha\beta} \epsilon_{\alpha\beta} = \frac{K}{2} (\nabla \cdot \mathbf{u})^2 + \frac{c_{11} - c_{12}}{2} \sum_{\alpha} \left(e_{\alpha\alpha} - \frac{1}{3} \nabla \cdot \mathbf{u} \right)^2 + c_{44} \sum_{\alpha \neq \beta} e_{\alpha\beta}^2 \quad (8)$$

TABLE I: Coefficients for cubic BaTiO₃. First line: c_{ij} (in GPa)[32] and $Q_{11}, Q_{12}, Q_{44}, Q_{11} - Q_{12}$, and $Q_{11} + 2Q_{12}$ (in m⁴/C²)[32], where $1 \text{ m}^4/\text{C}^2 \cong 0.11/\text{GPa}$. Second line: g_{ij} , and $M_{11}, M_{12}, M_{44}, M_{11} - M_{12}$, and $M_{11} + 2M_{12}$, where M_{ij} will be related to g_{ij} in Eq.(41).

c_{11}	c_{12}	c_{44}	Q_{11}	Q_{12}	Q_{44}	$Q_{11} - Q_{12}$	$Q_{11} + 2Q_{12}$
305	106	128	0.115	-0.033	0.041	0.148	0.049
g_{11}	g_{12}	g_{44}	M_{11}	M_{12}	M_{44}	$M_{11} - M_{12}$	$M_{11} + 2M_{12}$
4.28	-0.71	0.59	4.77	-1.04	0.041	5.81	2.69

where $\epsilon_{\alpha\beta} = (\nabla_\alpha u_\beta + \nabla_\beta u_\alpha)/2$ are the strains and $\sigma_{\alpha\beta}$ are the elastic stress components,

$$\sigma_{\alpha\beta} = \left[(c_{11} - c_{12})\epsilon_{\alpha\alpha} + c_{12} \sum_\gamma \epsilon_{\gamma\gamma} \right] \delta_{\alpha\beta} + 2c_{44}(\epsilon_{\alpha\beta} - \epsilon_{\alpha\alpha}\delta_{\alpha\beta}). \quad (9)$$

The c_{ij} are the bare (unrenormalized) elastic moduli and $K = (c_{11} + 2c_{12})/3$ is the bare bulk modulus, We suppose a reference equilibrium state above T_c in the stress-free boundary condition (or at a fixed low ambient pressure) without applied field, where the thermal averages of the strains $\langle \epsilon_{\alpha\beta} \rangle$ vanish. At long wavelengths, the mass density deviation $\delta\rho$ is related to the dilation strain $\nabla \cdot \mathbf{u}$ as [69]

$$\delta\rho = -\rho \nabla \cdot \mathbf{u} = -\rho \sum_\gamma \epsilon_{\gamma\gamma}, \quad (10)$$

where ρ is the average mass density and no vacancies are assumed in the crystal.

The f_{int} in Eq.(1) represents the ES coupling as

$$f_{\text{int}} = -\sum_{\alpha,\beta} \Pi_{\alpha\beta}^s \epsilon_{\alpha\beta} = -\sum_{\alpha,\beta} e_{\alpha\beta}^s \sigma_{\alpha\beta}. \quad (11)$$

Here, $\{\Pi_{\alpha\beta}^s\}$ is the singular stress tensor and $\{e_{\alpha\beta}^s\}$ is the singular strain tensor, which are bilinear in \mathbf{p} . For cubic solids they are expressed as [16, 28–33]

$$\Pi_{\alpha\beta}^s = [(g_{11} - g_{12})p_\alpha^2 + g_{12}|\mathbf{p}|^2]\delta_{\alpha\beta} + g_{44}(p_\alpha p_\beta - p_\alpha^2 \delta_{\alpha\beta}), \quad (12)$$

$$e_{\alpha\beta}^s = [(Q_{11} - Q_{12})p_\alpha^2 + Q_{12}|\mathbf{p}|^2]\delta_{\alpha\beta} + \frac{1}{2}Q_{44}(p_\alpha p_\beta - p_\alpha^2 \delta_{\alpha\beta}), \quad (13)$$

where g_{ij} and Q_{ij} are constants. In Voigt notation we have $\epsilon_1^s = \epsilon_{xx}^s$, $\epsilon_2^s = \epsilon_{yy}^s$, $\epsilon_3^s = \epsilon_{zz}^s$, $\epsilon_4^s = 2e_{yz}^s$, $\epsilon_5^s = 2e_{zx}^s$, and $\epsilon_6^s = 2e_{xy}^s$ [16, 32]. Since Eq.(11) holds for any $\epsilon_{\alpha\beta}$, we find

$$Q_{11} - Q_{12} = \frac{g_{11} - g_{12}}{c_{11} - c_{12}}, \quad Q_{11} + 2Q_{12} = \frac{g_{11} + 2g_{12}}{c_{11} + 2c_{12}}, \quad Q_{44} = \frac{g_{44}}{c_{44}}, \quad (14)$$

To derive these relations we set $\Pi_{\alpha\alpha}^s = (g_{11} - g_{12})\mathcal{D}_\alpha + (g_{11} + 2g_{12})|\mathbf{p}|^2/3$ and $e_{\alpha\alpha}^s = (Q_{11} - Q_{12})\mathcal{D}_\alpha + (Q_{11} + 2Q_{12})|\mathbf{p}|^2/3$ with $\mathcal{D}_\alpha = p_\alpha^2 - |\mathbf{p}|^2/3$ (see Eqs.(C4)-(C7)).

In Table 1, we present c_{ij} , Q_{ij} , and g_{ij} using theoretical values by Chen's group[32] for cubic BaTiO₃, where M_{ij} will be introduced in Sec.III. Their Q_{ij} values are consistent with measured values[28, 30, 33]. The Q_{ij} were also measured for KaTiO₃ [29]. They have been obtained from shape changes of single crystals with uniform polarization in unclamped samples. See Appendix A for more discussions on this aspect.

In addition, Landau and Lifshitz introduced the thermoelastic free energy density [69],

$$f_T = -K\alpha_P(T - T_{\text{ex}})\nabla \cdot \mathbf{u}, \quad (15)$$

where T_{ex} is the reference temperature above T_c , $K = (c_{11} + 2c_{12})/3$ is the bulk modulus, and $\alpha_P = -(\partial\rho/\partial T)_P/\rho$ is the thermal expansion coefficient. In α_P the ambient pressure P is fixed, which is equal to P_{ex} in the reference state. This P should not be confused with the polarization \mathbf{p} . Then, a temperature change δT from T_{ex} induces a density change $\delta\rho = -\rho\alpha_P\delta T$ in equilibrium at fixed P . The total stress tensor is written as

$$\Pi_{\alpha\beta}^{\text{tot}} = -\sigma_{\alpha\beta} + \Pi_{\alpha\beta}^s + [K\alpha_P(T - T_{\text{ex}}) + P_{\text{ex}}]\delta_{\alpha\beta}. \quad (16)$$

We also define the internal pressure \hat{P} by

$$\hat{P} = \sum_{\alpha} \Pi_{\alpha\alpha}^{\text{tot}}/3 = -K\nabla \cdot \mathbf{u} + (g_{11} + 2g_{12})|\mathbf{p}|^2/3 + K\alpha_P(T - T_{\text{ex}}) + P_{\text{ex}}. \quad (17)$$

We have the thermal averages $\langle \Pi_{\alpha\beta}^{\text{tot}} \rangle = \langle \hat{P} \rangle \delta_{\alpha\beta} = P\delta_{\alpha\beta}$ in equilibrium unclamped samples.

In the paraelectric phase without anisotropic strains we can define the thermodynamic entropy $s(T, P)$ per unit mass and use the Maxwell relations [70–72]. Then, we find the thermodynamic relations $K = \rho(\partial P/\partial\rho)_T$ and $K\alpha_P = (\partial P/\partial T)_\rho$ [69]. For example, in longitudinal sounds, T adiabatically varies by $-\rho(\partial T/\partial\rho)_s\nabla \cdot \mathbf{u}$. Then, in Eq.(17), the isothermal bulk modulus K is replaced by the adiabatic one [69],

$$K_{\text{ad}} = K[1 - (\partial\rho/\partial T)_P(\partial T/\partial\rho)_s] = K\gamma = \rho(\partial P/\partial\rho)_s, \quad (18)$$

where $c_{11} - c_{12}$ and c_{44} are unchanged. Here, $\gamma = C_P/C_V$ is the specific heat ratio, which is very close to 1 for most solids (including BaTiO₃). Thus, we will set $K_{\text{ad}} = K$ in Sec.IV.

2.4. Functional derivatives and dielectric constant of films

From Eqs.(1), (2), and (16) the functional derivatives of \mathcal{F} are given by

$$\left(\frac{\delta\mathcal{F}}{\delta\mathbf{p}}\right)\mathbf{u} = -\mathbf{E} - C\nabla^2\mathbf{p} + \left(\frac{\partial(f_B + f_{\text{int}})}{\partial\mathbf{p}}\right)\mathbf{u}, \quad (19)$$

$$\left(\frac{\delta\mathcal{F}}{\delta u_\alpha}\right)\mathbf{p} = \sum_\beta \nabla_\beta \Pi_{\alpha\beta}^{\text{tot}} = -\sum_\beta \nabla_\beta \sigma_{\alpha\beta} + \sum_\beta \nabla_\beta \Pi_{\alpha\beta}^s + K\alpha_P \nabla_\alpha T, \quad (20)$$

which vanish for the equilibrium averages of \mathbf{p} and \mathbf{u} . The last term in Eq.(20) is negligible for homogeneous T and in discussing sounds (see below Eq.(18)).

We also remark on the finite-size effect in the observed dielectric constant ϵ_{eff} of films [3, 73–79]. Let us suppose thin surface layers with a thickness $d_s (\ll H)$ and a low dielectric constant $\epsilon_s (\ll \epsilon)$ in the presence of surface charges $\pm Q_0$ at $z = 0$ and H . In this situation, the electric field in the layers E_s is much larger than the bulk field E_b from $\epsilon_s E_s = \epsilon E_b = D_z = 4\pi Q_0/L^2$. Defining ϵ_{eff} by $\Phi_a = \int_0^H dz E_z(z) = HD_z/\epsilon_{\text{eff}}$, we obtain

$$1/\epsilon_{\text{eff}} = [(H - 2d)/\epsilon + 2d/\epsilon_s]/H = 1/\epsilon + 2\ell_s/H, \quad (21)$$

where $\ell_s = d_s/(\epsilon_s - 1/\epsilon) \cong d_s/\epsilon_s$, $\epsilon_{\text{eff}} \cong H/2\ell_s$ for $\epsilon > H/2\ell_s$, and $E_b = \Phi_a/(H + 2\ell_s)$. See Eq.(60) for an effective frequency-dependent dielectric constant of films. We note that Eq.(21) can be derived from the Kretschmer-Binder surface free energy in the Ginzburg-Landau scheme [19, 80]. For ferroelectrics, the observed size of ℓ_s depends on the experimental conditions and its origin has long been discussed[77–79]. In electrochemistry the combination $C_s = 1/4\pi\ell_s = \epsilon_s/4\pi d_s$ is called the surface capacitance [81]. We point out that the effective dielectric constant of polar fluids depends on the film thickness H in the same manner[68, 82–84] due to the Stern layers with a microscopic width at metal-water interfaces [81], which was confirmed experimentally for nanoconfined liquid water [85].

3. Correlations in Fourier space

3.1. Ginzburg criterion and mean-field approximation

In calculating the polarization correlations for $T > T_c$, we can treat the fourth order terms in Eq.(1) as a perturbation. Their contributions are small corrections for $A > A_{\text{Gi}}$ (see Eq.(4.125) in Ref.18). The lower bound A_{Gi} is calculated as [13, 18, 35, 86]

$$A_{\text{Gi}} = (a_{4\text{th}} k_B T / 2\pi^2)^2 / C^3, \quad (22)$$

where $a_{4\text{th}}$ is the largest value of the coefficients of the fourth order terms in f_B . For $A > A_{\text{Gi}}$ we can use the mean-field theory, where the polarization fluctuations obey the

Gaussian distribution. For BaTiO₃, A_{Gi} is extremely small [13]. In fact, $A_{\text{Gi}} \sim 10^{-6}$ if $a_{4\text{th}}$ is set equal to a_{12} in the work by Li *et al.* [31]. It increases up to 10^{-5} if $a_{4\text{th}}$ is equated to β_1 in Eq.(A5) in Appendix A. Here, we assume $\sqrt{C} \cong 1.5 \text{ \AA}$ (see Eq.(50)). It is known that BaTiO₃ at low pressures is close to a tricritical point in the P - T phase diagram [9–12].

3.2. Fourier components and polarization correlation

We consider the thermal fluctuations of \mathbf{p} and \mathbf{u} in the bulk region far from the surfaces without applied field, where the translational symmetry nearly holds. Their statistical distribution is proportional to $\exp(-\mathcal{F}(\{\mathbf{p}\}, \{\mathbf{u}\})/k_B T)$. Hereafter, $\langle \cdots \rangle$ denotes the equilibrium average. We calculate the correlations for the Fourier components of \mathbf{p} and \mathbf{u} ,

$$\hat{\mathbf{p}}(\mathbf{q}) = \int d\mathbf{r} e^{-i\mathbf{q}\cdot\mathbf{r}} \mathbf{p}(\mathbf{r}), \quad \hat{\mathbf{u}}(\mathbf{q}) = \int d\mathbf{r} e^{-i\mathbf{q}\cdot\mathbf{r}} \mathbf{u}(\mathbf{r}), \quad (23)$$

where $\mathbf{q} = 2\pi(n_x/L, n_y/L, n_z/H)$ with (n_x, n_y, n_z) being integers for our $L \times L \times H$ system. The wave number $q = |\mathbf{q}|$ is in the range $2\pi/H \leq q < \pi/d$. It is convenient to divide $\hat{\mathbf{p}}(\mathbf{q})$ into the longitudinal part $\hat{\mathbf{p}}_{\parallel} = (\hat{\mathbf{p}} \cdot \hat{\mathbf{q}})\hat{\mathbf{q}}$ and the transverse part $\hat{\mathbf{p}}_{\perp} = \hat{\mathbf{p}} - \hat{\mathbf{p}}_{\parallel}$, where $\hat{\mathbf{q}} = q^{-1}\mathbf{q}$.

We consider the contribution to \mathcal{F} from the Fourier components with $\mathbf{q} \neq \mathbf{0}$, retaining the bilinear terms and the third order ES term. The resultant free energy is then divided into two parts as $\mathcal{F}_{\text{inh}} = \mathcal{F}_{\text{inh}}^{\text{po}} + \mathcal{F}_{\text{inh}}^{\text{el}}$, where

$$\mathcal{F}_{\text{inh}}^{\text{po}} = \frac{1}{2V} \sum_{\mathbf{q} \neq \mathbf{0}} \left[4\pi \hat{\mathbf{p}}_{\parallel}(\mathbf{q})|^2 + (A + Cq^2) |\hat{\mathbf{p}}(\mathbf{q})|^2 \right], \quad (24)$$

$$\mathcal{F}_{\text{inh}}^{\text{el}} = \frac{1}{V} \sum_{\mathbf{q} \neq \mathbf{0}, \alpha, \beta} \left[\frac{1}{2} q^2 Z_{\alpha\beta}(\hat{\mathbf{q}}) \hat{u}_{\alpha}(\mathbf{q}) \hat{u}_{\beta}(\mathbf{q})^* - \hat{\Pi}_{\alpha\beta}^{\text{s}}(\mathbf{q})^* i q_{\beta} \hat{u}_{\alpha}(\mathbf{q}) \right]. \quad (25)$$

In Eq.(24), the Fourier component of \mathbf{E} is set equal to $-4\pi\hat{\mathbf{p}}_{\parallel}$ from $\nabla \cdot \mathbf{E} = -\nabla^2 \Phi = -4\pi \nabla \cdot \mathbf{p}$, where the surface effect is neglected. In Eq.(25), $\sum_{\beta} q^2 Z_{\alpha\beta}(\hat{\mathbf{q}}) \hat{u}_{\beta}(\mathbf{q})$ is the Fourier component of $-\sum_{\beta} \nabla_{\beta} \sigma_{\alpha\beta}$, while $\hat{\Pi}_{\alpha\beta}^{\text{s}}(\mathbf{q})$ is that of $\Pi_{\alpha\beta}^{\text{s}}$. The $\{Z_{\alpha\beta}\}$ is called the Christoffel matrix [87]:

$$Z_{\alpha\beta}(\hat{\mathbf{q}}) = a_{\alpha} \delta_{\alpha\beta} + (c_{12} + c_{44}) \hat{q}_{\alpha} \hat{q}_{\beta}, \quad (26)$$

$$a_{\alpha}(\hat{\mathbf{q}}) = c_{44} + (c_{11} - c_{12} - 2c_{44}) \hat{q}_{\alpha}^2. \quad (27)$$

From Eq.(24) we obtain the polarization correlation [68],

$$G_{\alpha\beta}(\mathbf{q}) = \langle \hat{p}_{\alpha}(\mathbf{q}) \hat{p}_{\beta}(\mathbf{q})^* \rangle \frac{1}{Vk_B T} = \frac{\hat{q}_{\alpha} \hat{q}_{\beta}}{A + 4\pi + Cq^2} + \frac{\delta_{\alpha\beta} - \hat{q}_{\alpha} \hat{q}_{\beta}}{A + Cq^2} \quad (\mathbf{q} \neq \mathbf{0}). \quad (28)$$

The second term is the variance of $\hat{\mathbf{p}}_{\perp}$, which grows for $q\xi \lesssim 1$ and $A \ll 1$ with ξ being given in Eq.(7). Thus, $\hat{\mathbf{p}}_{\perp}$ exhibits the critical fluctuations, while the longitudinal part $\hat{\mathbf{p}}_{\parallel}$ is

suppressed by the dipolar interaction. In the real space, the inverse Fourier transforms of the two terms in Eq.(28) decay exponentially as $\exp[-r\sqrt{4\pi/C}]$ and $\exp[-r/\xi]$, respectively. Aharony and Fisher[88] started with Eq.(28) to study the asymptotic critical behavior of isotropic dipolar systems. For uniaxial non-piezoelectric systems such as TGS, the z component p_z is the single order parameter with the angle-dependent variance [25, 26, 37, 38],

$$\langle \hat{p}_z(\mathbf{q})\hat{p}_z(\mathbf{q})^* \rangle / V = k_B T / (A + Cq^2 + 4\pi\hat{q}_z^2),$$

where $4\pi\hat{q}_z^2$ in the denominator arises from the dipolar interaction.

From Eq.(3) the singular energy density is given by $e_{\text{sing}} = f_B - T\partial f_B/\partial T = -a_1|\mathbf{p}|^2/2$ in the lowest order in \mathbf{p} . Then, for $T > T_c$, we obtain the singular specific heat [5, 89],

$$C_{\text{sing}} = \frac{\partial}{\partial T} \langle e_{\text{sing}} \rangle = \frac{a_1^2}{4k_B T^2} \int d\mathbf{r} \langle \delta|\mathbf{p}|^2(\mathbf{r})\delta|\mathbf{p}|^2(\mathbf{0}) \rangle = \frac{a_1^2}{4T} I_e A^{-1/2}, \quad (29)$$

where we use the decoupling approximation with Eq.(28). The coefficient I_e is defined by

$$I_e = k_B T / [2\pi C^{3/2}], \quad (30)$$

where C is the coefficient in the gradient free energy. Here, the factor $a_1^2/4$ is extremely small, so the higher order terms in the free energy can well exceed the above C_{sing} . Experimentally, the specific heat singularity in cubic BaTiO₃ has been very small [5, 89, 90]. To derive Eq.(29) systematically we can introduce the fluctuating energy density variable e with the coupling $\propto e|\mathbf{p}|^2$ in \mathcal{F} [18, 91]. Note that the four-body correlation in Eq.(29) grows nearly logarithmically as $\log A^{-1}$ in the asymptotic critical regime [18, 91].

3.3. Correlations of acoustic and electrostrictive displacements

Accounting for the ES coupling in Eq.(11), we divide the Fourier component $\hat{u}_\alpha(\mathbf{q})$ as

$$\hat{m}_\alpha(\mathbf{q}) = -\frac{1}{q^2} \sum_{\beta,\gamma} Z^{\alpha\beta}(\hat{\mathbf{q}}) i q_\gamma \hat{\Pi}_{\beta\gamma}^s(\mathbf{q}), \quad \hat{w}_\alpha(\mathbf{q}) = \hat{u}_\alpha(\mathbf{q}) - \hat{m}_\alpha(\mathbf{q}) \quad (\mathbf{q} \neq \mathbf{0}). \quad (31)$$

Here, $\hat{m}_\alpha(\mathbf{q})$ is the ES part consisting of the Fourier components of the bilinear terms $\propto p_\beta p_\gamma$, while $\hat{w}_\alpha(\mathbf{q})$ is the acoustic part. The matrix $\{Z^{\alpha\beta}(\hat{\mathbf{q}})\}$ is the inverse of $\{Z_{\alpha\beta}(\hat{\mathbf{q}})\}$ [16, 17, 92]:

$$Z^{\alpha\beta}(\hat{\mathbf{q}}) = \frac{\delta_{\alpha\beta}}{a_\alpha(\hat{\mathbf{q}})} - \frac{(c_{12} + c_{44})\hat{q}_\alpha\hat{q}_\beta}{a_\alpha(\hat{\mathbf{q}})a_\beta(\hat{\mathbf{q}})(1 + b(\hat{\mathbf{q}}))}, \quad (32)$$

$$b(\hat{\mathbf{q}}) = (c_{12} + c_{44}) \sum_\gamma \hat{q}_\gamma^2 / a_\gamma(\hat{\mathbf{q}}), \quad (33)$$

where $b(\hat{\mathbf{q}}) = 3.30$ for $\hat{\mathbf{q}}$ along [001] from Table 1. In Sec.IV, we shall see that \hat{m}_α and \hat{w}_α evolve in time very differently, resulting in the central and acoustic peaks, respectively.

In the real space, we have $m_\alpha(\mathbf{r}) = u_\alpha(\mathbf{r}) - w_\alpha(\mathbf{r}) = \sum_{\mathbf{q} \neq \mathbf{0}} e^{i\mathbf{q} \cdot \mathbf{r}} \hat{m}_\alpha(\mathbf{q})/V$. If \mathbf{r} is in the bulk region, we obtain the integral expression,

$$m_\alpha(\mathbf{r}) = -\sum_{\beta, \gamma} \int d\mathbf{r}' \mathcal{K}_{\alpha\beta}(\mathbf{r} - \mathbf{r}') \nabla'_\gamma \Pi_{\beta\gamma}^s(\mathbf{r}'). \quad (34)$$

Here, $\mathcal{K}_{\alpha\beta}(\mathbf{r})$ are the Green functions in the limit $V \rightarrow \infty$ given by

$$\mathcal{K}_{\alpha\beta}(\mathbf{r}) = \frac{1}{(2\pi)^3} \int d\mathbf{q} e^{i\mathbf{q} \cdot \mathbf{r}} \frac{1}{q^2} Z^{\alpha\beta}(\hat{\mathbf{q}}) = \frac{1}{8\pi^2 r} \int d\theta d\varphi \sin\theta Z^{\alpha\beta}(\hat{\mathbf{q}}) \delta(\hat{\mathbf{q}} \cdot \hat{\mathbf{r}}). \quad (35)$$

where $\int d\theta d\varphi \sin\theta(\dots)$ is the angle integration of $\hat{\mathbf{q}}$. The delta function $\delta(\hat{\mathbf{q}} \cdot \hat{\mathbf{r}})$ follows from $Z^{\alpha\beta}(-\hat{\mathbf{q}}) = Z^{\alpha\beta}(\hat{\mathbf{q}})$, where $\hat{\mathbf{r}} = r^{-1}\mathbf{r}$. Thus, $r\mathcal{K}_{\alpha\beta}(\mathbf{r})$ depends only on $\hat{\mathbf{r}}$. If $\hat{\mathbf{r}} = (0, 0, 1)$, we have $r\mathcal{K}_{\alpha\beta}(\hat{\mathbf{r}}) = \int_0^{2\pi} d\varphi Z^{\alpha\beta}(\hat{\mathbf{q}})/8\pi^2$ with $\hat{\mathbf{q}} = (\cos\varphi, \sin\varphi, 0)$. We note that the elastic field around an impurity can be expressed in terms of $\mathcal{K}_{\alpha\beta}(\mathbf{r})$ in cubic solids.

With the division of the displacement in Eq.(31), $\mathcal{F}_{\text{inh}}^{\text{el}}$ in Eq.(25) is rewritten as

$$\mathcal{F}_{\text{inh}}^{\text{el}} = \frac{1}{2V} \sum_{\mathbf{q} \neq \mathbf{0}, \alpha, \beta} q^2 Z_{\alpha\beta}(\hat{\mathbf{q}}) \hat{w}_\alpha(\mathbf{q}) \hat{w}_\beta(\mathbf{q})^* + \Delta\mathcal{F}_{\text{inh}}^{\text{el}}(\{\mathbf{p}\}), \quad (36)$$

where $\Delta\mathcal{F}_{\text{inh}}^{\text{el}}$ depends only on \mathbf{p} as will be shown in Eq.(51). The variables $\hat{w}_\alpha(\mathbf{q})$ and $\hat{p}_\alpha(\mathbf{q})$ are statistically independent of each other. Thus, the displacement correlation, written as $U_{\alpha\beta}(\mathbf{q})$, is divided into those of \hat{w}_α and \hat{m}_α as

$$\begin{aligned} U_{\alpha\beta}(\mathbf{q}) &= \langle \hat{u}_\alpha(\mathbf{q}) \hat{u}_\beta(\mathbf{q})^* \rangle / V = \langle \hat{w}_\alpha(\mathbf{q}) \hat{w}_\beta(\mathbf{q})^* \rangle / V + \langle \hat{m}_\alpha(\mathbf{q}) \hat{u}_\beta(\mathbf{q})^* \rangle / V \\ &= k_B T Z^{\alpha\beta}(\hat{\mathbf{q}}) / q^2 + R_{\alpha\beta}(\mathbf{q}). \end{aligned} \quad (37)$$

The ES correlation $R_{\alpha\beta}(\mathbf{q})$ is written in terms of the stress correlation $\Psi_{\alpha\beta}(\mathbf{q})$ as

$$R_{\alpha\beta}(\mathbf{q}) = \frac{1}{q^2} k_B T \sum_{\gamma, \nu} Z^{\alpha\gamma}(\hat{\mathbf{q}}) Z^{\beta\nu}(\hat{\mathbf{q}}) \Psi_{\gamma\nu}(\mathbf{q}). \quad (38)$$

$$\Psi_{\alpha\beta}(\mathbf{q}) = \frac{1}{k_B T} \sum_{\gamma, \nu} \hat{q}_\gamma \hat{q}_\nu \int d\mathbf{r} e^{-i\mathbf{q} \cdot \mathbf{r}} \langle \delta\Pi_{\alpha\gamma}^s(\mathbf{r}) \delta\Pi_{\beta\nu}^s(\mathbf{0}) \rangle, \quad (39)$$

where $\delta\Pi_{\alpha\gamma}^s = \Pi_{\alpha\gamma}^s - \langle \Pi_{\alpha\gamma}^s \rangle$. Hereafter, to avoid cumbersome notation, we will write $Z_{\alpha\beta}(\hat{\mathbf{q}})$, $a_\alpha(\hat{\mathbf{q}})$, $Z^{\alpha\beta}(\hat{\mathbf{q}})$, and $b(\hat{\mathbf{q}})$ as $Z_{\alpha\beta}$, a_α , $Z^{\alpha\beta}$, and b unless confusion may occur.

In this paper, we use $\Psi_{\alpha\beta}(\mathbf{q})$ in the limit $q \rightarrow 0$ assuming $q\xi \ll 1$. Then, in Eq.(39), $e^{-i\mathbf{q} \cdot \mathbf{r}}$ can be set equal to 1 because the integrand decays exponentially ($\propto e^{-2r/\xi}$). However, $\Psi_{\alpha\beta}(\mathbf{q})$ still depends on $\hat{\mathbf{q}}$ because of the factor $\hat{q}_\gamma \hat{q}_\nu$. In Appendix C, we will find that $\Psi_{\alpha\beta}(\hat{\mathbf{q}}) = \lim_{q \rightarrow 0} \Psi_{\alpha\beta}(\mathbf{q})$ grows as $A^{-1/2}$ in the following form,

$$\Psi_{\alpha\beta}(\hat{\mathbf{q}}) = \left[(M_{44} + (M_{11} - M_{12} - 2M_{44})\hat{q}_\alpha^2) \delta_{\alpha\beta} + (M_{12} + M_{44})\hat{q}_\alpha \hat{q}_\beta \right] I_e A^{-1/2}. \quad (40)$$

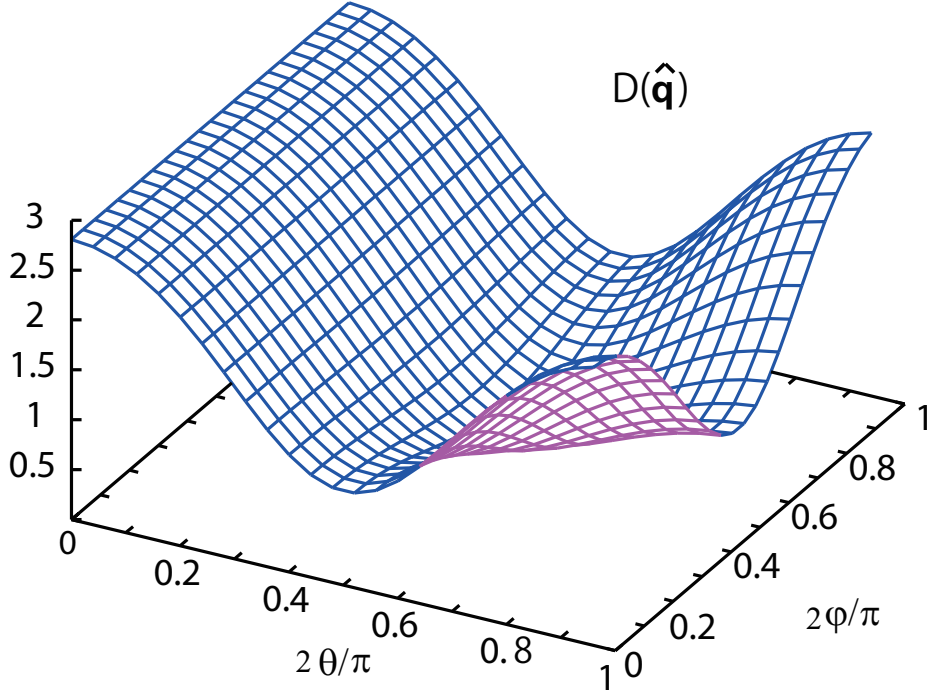


FIG. 1: Anisotropy factor $D(\hat{\mathbf{q}})$ in Eqs.(42) and (43) in the density correlation for cubic BaTiO₃ as a function of (θ, φ) with $\hat{\mathbf{q}} = (\sin \theta \cos \varphi, \sin \theta \sin \varphi, \cos \theta)$. Its maximum is 2.8, which is attained at $\theta = 0$ ([001]), $(\theta, \varphi) = (\pi/2, 0)$ ([100]), and $(\theta, \varphi) = (\pi/2, \pi/2)$ ([010]). Its minimum is 0.44 for $(\theta, \varphi) = (\pi/4, \pi/4)$ ([111]). Use is made of c_{ij} and M_{ij} in Table 1.

In terms of g_{ij} in Eq.(12), the dimensionless coefficients M_{ij} are given by

$$M_{11} - M_{12} = 7(g_{11} - g_{12})^2/30, \quad M_{11} + 2M_{12} = (g_{11} + 2g_{12})^2/3, \quad M_{44} = 7g_{44}^2/60. \quad (41)$$

In Table 1 we give M_{ij} for BaTiO₃, where $M_{11} - M_{12}$ is the largest combination and M_{44} is very small. Thus, $\Psi_{\alpha\beta}(\hat{\mathbf{q}}) \cong (M_{11} - M_{12})\hat{q}_\alpha^2\delta_{\alpha\beta}I_e A^{-1/2}$. From the cubic symmetry, $Z_{\alpha\beta}(\mathbf{q})$ in Eq.(26) and $\Psi_{\alpha\beta}(\hat{\mathbf{q}})$ in Eq.(40) assume the same tensorial form.

3.4. Density correlation and entropy fluctuation

From Eq.(10) we have $\hat{\rho}(\mathbf{q}) = \int d\mathbf{r} e^{-i\mathbf{q}\cdot\mathbf{r}} \delta\rho(\mathbf{r}) = -\rho i\mathbf{q} \cdot \hat{\mathbf{u}}(\mathbf{q})$. Then, Eq.(37) gives

$$\begin{aligned} I_D(\mathbf{q}) &= \langle |\hat{\rho}(\mathbf{q})|^2 \rangle / V \rho^2 = \sum_{\alpha,\beta} q_\alpha q_\beta U_{\alpha\beta}(\mathbf{q}) \\ &= \frac{k_B T b(\hat{\mathbf{q}})}{(c_{12} + c_{44})(1 + b(\hat{\mathbf{q}}))} + \frac{k_B T I_e}{(c_{12} + c_{44})^2} D(\hat{\mathbf{q}}) A^{-1/2}. \end{aligned} \quad (42)$$

In the second line, the first term is the variance of $-i\mathbf{q} \cdot \hat{\mathbf{u}}(\mathbf{q})$ and the second term is that of $-i\mathbf{q} \cdot \hat{\mathbf{m}}(\mathbf{q})$. The first term becomes $k_B T / c_{11}$ for $\hat{\mathbf{q}}$ along [001]. From $\sum_\gamma Z^{\alpha\gamma} \hat{q}_\gamma =$

$\hat{q}_\alpha/[a_\alpha(1+b)]$. we express the factor $D(\hat{\mathbf{q}})$ in the second term as

$$D(\hat{\mathbf{q}}) = \frac{(c_{12} + c_{44})^2}{k_B T I_e} \sum_{\alpha, \beta} \hat{q}_\alpha \hat{q}_\beta R_{\alpha\beta} = \frac{b^2}{(1+b)^2} (M_{12} + M_{44}) + \frac{(c_{12} + c_{44})^2}{(1+b)^2} \sum_{\gamma} \frac{\hat{q}_\gamma^2}{a_\gamma^2} [M_{44} + (M_{11} - M_{12} - 2M_{44})\hat{q}_\gamma^2], \quad (43)$$

where $b(\hat{\mathbf{q}})$ is written as b . In Fig.1, we display $D(\hat{\mathbf{q}})$ for cubic BaTiO₃. Its maximum is $D[001] = 2.8$ along $[001]$ and its minimum is $D[111] = 0.44$ along $[111]$, while it is $D[110] = 0.94$ along $[011]$. The ratio of the second term to the first one in Eq.(42) is about $0.4 \times 10^{-2} A^{-1/2}$ along $[001]$. which increases up to 0.1 at $T = T_c$ for BaTiO₃.

In $I_D(\mathbf{q})$ in Eq.(42) the contribution from the entropy fluctuation $\delta s(\mathbf{r})$ (per unit mass) is omitted, which is crucial for compressible fluids [18, 93, 94]. Note that the isobaric part of the density deviation $(\partial\rho/\partial s)_p \delta s$ contributes $k_B T^2 \alpha_P^2 / C_P$ to $I_D(\mathbf{q})$, which is the integral intensity of the Rayleigh scattering. Here, the first term in Eq.(42) is of order $k_B T / c_{11} \sim k_B T (\partial\rho/\partial P)_s / \rho$ from Eq.(18). Thus, in Eq.(42), the omitted entropy contribution is smaller than the first term by a factor of the Landau-Placzek ratio [4],

$$\gamma - 1 = C_P / C_V - 1 = (c_{11} + 2c_{12}) T \alpha_P^2 / 3C_P, \quad (44)$$

where $\gamma - 1 \sim 2.5 \times 10^{-3}$ for BaTiO₃ with C_P and C_V being the isobaric and isochoric specific heats per unit volume, respectively. We also find $\gamma - 1 \sim 10^{-2}$ for KDP and $\gamma - 1 \sim 10^{-3}$ for TGS. However, some experimental groups [49, 50, 57] ascribed the origin of the central peak near the ferroelectric transition to the Rayleigh scattering.

3.5. Elastic free energy in terms of renormalized elastic moduli C_{ij}

Let us integrate the statistical distribution over \mathbf{p} at fixed \mathbf{u} as

$$\int d\{\mathbf{p}\} \exp[-\mathcal{F}(\{\mathbf{p}\}, \{\mathbf{u}\})/k_B T] = \text{const.} \exp \left[-\frac{1}{2V} \sum_{\mathbf{q} \neq \mathbf{0}, \alpha, \beta} U^{\alpha\beta}(\mathbf{q}) \hat{u}_\alpha(\mathbf{q}) \hat{u}_\beta(\mathbf{q})^* \right], \quad (45)$$

where $\int d\{\mathbf{p}\}(\dots)$ denotes the functional integration and we consider the distribution of $\hat{u}_\alpha(\mathbf{q})$ with $\hat{\mathbf{q}} \neq \mathbf{0}$. Here, $\{U^{\alpha\beta}(\mathbf{q})\}$ is the inverse matrix of $\{U_{\alpha\beta}(\mathbf{q})\}$ in Eq.(37). We can then define the renormalized, static elastic moduli C_{ij} by

$$U^{\alpha\beta}(\mathbf{q}) = \left[(C_{44} + (C_{11} - C_{12} - 2C_{44})\hat{q}_\alpha^2) \delta_{\alpha\beta} + (C_{12} + C_{44})\hat{q}_\alpha \hat{q}_\beta \right] q^2 / k_B T, \quad (46)$$

where c_{ij} in $Z_{\alpha\beta}$ in Eq.(26) are replaced by C_{ij} in Eq.(46). Since Eqs.(37) and (38) give $U_{\alpha\beta} q^2 / k_B T = Z^{\alpha\beta} + \sum_{\gamma, \nu} Z^{\alpha\gamma} \Psi_{\gamma\nu} Z^{\nu\beta}$, we can expand $U^{\alpha\beta}(\mathbf{q})$ with respect to $\Psi_{\alpha\beta}(\mathbf{q})$ as

$$U^{\alpha\beta}(\mathbf{q}) = [Z_{\alpha\beta} - \Psi_{\alpha\beta}(\mathbf{q}) + \dots] q^2 / k_B T. \quad (47)$$

Then, to linear order in $\Psi_{\alpha\beta}(\mathbf{q})$, Eqs.(26), (27), (40), (46), and (47) give

$$C_{ij} = c_{ij} - M_{ij}I_e A^{-1/2}. \quad (48)$$

The renormalized frequency-dependent elastic moduli will be given in Eq.(78),

From Eq.(48) we find $\Delta C_{11}/c_{11} = 1 - C_{11}/c_{11} = 2.2 \times 10^{-4}(d/\sqrt{C})^3 A^{-1/2}$ with $d = 4 \text{ \AA}$, where we use c_{11} and M_{11} in Table 1. Experimentally, Kashida *et al.* [40] found

$$\Delta C_{11}/c_{11} = 0.032(T/T_0 - 1)^{-1.2} = 0.43 \times 10^{-2} A^{-1/2}. \quad (49)$$

We equate our theoretical expression to the above experimental one to determine the coefficient C in the gradient free energy as

$$\sqrt{C} = 1.5 \text{ \AA}. \quad (50)$$

Then, $\xi = 1.5A^{-1/2} \text{ \AA} = 11(T/T_0 - 1)^{-1/2} \text{ \AA}$ from Eq.(6a).

Li *et al.*[41] determined all ΔC_{ij} in cubic BaTiO₃ by Brillouin scattering, where $\Delta C_{11}/c_{11} \sim 0.1$ and $\Delta C_{44}/c_{44} \sim 0.02$ at $T = T_c$. Their findings agree with Eq.(49) and M_{ij} in Table 1. Thus, these previous results [32, 40, 41] justify the expansion of $U^{\alpha\beta}(\mathbf{q})$ with respect to $\Psi_{\alpha\beta}(\mathbf{q})$ in Eq.(47).

3.6. Free energy of \mathbf{p} after removal of \mathbf{u}

The free energy contribution from the inhomogeneous ES displacement $\hat{\mathbf{m}}(\mathbf{q})$ becomes

$$\begin{aligned} \Delta \mathcal{F}_{\text{inh}}^{\text{el}} &= -\frac{1}{2V} \sum_{\mathbf{q} \neq \mathbf{0}, \alpha, \beta, \gamma, \nu} Z^{\alpha\beta}(\hat{\mathbf{q}}) \hat{q}_\gamma \hat{q}_\nu \hat{\Pi}_{\alpha\gamma}^{\text{s}}(\mathbf{q}) \hat{\Pi}_{\beta\nu}^{\text{s}}(\mathbf{q})^* \\ &= -\frac{1}{2} \int d\mathbf{r} \int d\mathbf{r}' \sum_{\alpha, \gamma, \beta, \nu} \mathcal{K}_{\alpha\beta}(\mathbf{r} - \mathbf{r}') \nabla_\gamma \Pi_{\alpha\gamma}^{\text{s}}(\mathbf{r}) \cdot \nabla'_\nu \Pi_{\beta\nu}^{\text{s}}(\mathbf{r}'), \end{aligned} \quad (51)$$

which is the second term in Eq.(36). In the second line, we use $\mathcal{K}_{\alpha\beta}(\mathbf{r})$ in Eq.(35) neglecting the surface effect. After removal of \mathbf{u} we obtain the free energy of \mathbf{p} in the form,

$$\mathcal{F}_R(\{\mathbf{p}\}) = \int d\mathbf{r} \left[\frac{1}{8\pi} |\mathbf{E}|^2 + f_B \right] + \Delta \mathcal{F}_{\text{inh}}^{\text{el}} + \Delta \mathcal{F}_{\text{hom}}^{\text{el}}. \quad (52)$$

Here, $\Delta \mathcal{F}_{\text{hom}}^{\text{el}}$ arises from homogeneous strains in the stress-free boundary condition (or at a fixed ambient pressure) in unclamped samples, as will be derived in Appendix A.

We make comments. (i) For cubic perovskites, Nambu and Sagara [16] solved the dynamic equation $\tau_0 \partial \mathbf{p} / \partial t = -\delta \mathcal{F}_R / \delta \mathbf{p}$ (see Eq.(53)) after lowering T below T_0 in two dimensions, In \mathcal{F}_R they included $\Delta \mathcal{F}_{\text{inh}}^{\text{el}}$ and found its relevance in phase ordering. However, they set

$\Delta\mathcal{F}_{\text{hom}}^{\text{el}} = 0$ in the periodic boundary condition and $\mathbf{E} = \mathbf{0}$ without the dipolar interaction.

(ii) In phase-separating binary alloys forming a cubic crystal, the composition $\phi(\mathbf{r})$ is the order parameter with the Vegard coupling $g\phi\nabla \cdot \mathbf{u}$ in the free energy, where g is a constant [18, 95]. In this case, we can use Eq.(51) to obtain $\Delta\mathcal{F}_{\text{inh}}^{\text{el}} = \sum_{\mathbf{q} \neq \mathbf{0}} r_{\text{el}}(\hat{\mathbf{q}}) |\hat{\phi}(\mathbf{q})|^2 / 2V$, where $\hat{\phi}(\mathbf{q})$ is the Fourier component of $\phi(\mathbf{r})$ and

$$r_{\text{el}}(\hat{\mathbf{q}}) = -g^2 \sum_{\alpha, \beta} Z^{\alpha\beta}(\hat{\mathbf{q}}) \hat{q}_\alpha \hat{q}_\beta = -g^2 b(\hat{\mathbf{q}}) / [(1 + b(\hat{\mathbf{q}}))(c_{12} + c_{44})].$$

The $\hat{\mathbf{q}}$ -dependence of $\tau_{\text{el}}(\hat{\mathbf{q}})$ determines the domain structure in phase ordering.

4. Dynamics of \mathbf{p} and \mathbf{u}

4.1. Polarization time-correlation and frequency-dependent dielectric constant

Now, we examine dynamics of $\mathbf{p}(\mathbf{r}, t)$ and $\mathbf{u}(\mathbf{r}, t)$, which depend on space and time. Starting with Eq.(19) we set up the relaxation equation in the linear regime [16–18, 24, 68, 96],

$$\tau_0 \frac{\partial}{\partial t} \mathbf{p} = - \left(\frac{\delta \mathcal{F}}{\delta \mathbf{p}} \right)_{\mathbf{u}} = \mathbf{E} + C \nabla^2 \mathbf{p} - A \mathbf{p}, \quad (53)$$

where τ_0 is a microscopic time (to be estimated below Eq.(71)) and the nonlinear terms in the functional derivative in Eq.(19) are omitted. In Eq.(53) we also neglect the rapidly relaxing background polarization (such as the electronic one) [2, 100, 101].

We set the Fourier component of \mathbf{E} equal to $-4\pi \hat{\mathbf{p}}_{\parallel}$ for $\mathbf{q} \neq \mathbf{0}$ from $\nabla \cdot \mathbf{D} = 0$ in Eq.(53) to examine the bulk correlations. Then, the longitudinal part $\hat{\mathbf{p}}_{\parallel}$ and the transverse part $\hat{\mathbf{p}}_{\perp}$ of the Fourier component $\hat{\mathbf{p}}$ obey

$$\frac{\partial}{\partial t} \hat{\mathbf{p}}_{\parallel} = -\Gamma_{\parallel}(q) \hat{\mathbf{p}}_{\parallel}, \quad \frac{\partial}{\partial t} \hat{\mathbf{p}}_{\perp} = -\Gamma_{\perp}(q) \hat{\mathbf{p}}_{\perp} \quad (\mathbf{q} \neq \mathbf{0}),$$

where the longitudinal and transverse decay rates are given by

$$\Gamma_{\parallel}(q) = (A + 4\pi + Cq^2) / \tau_0, \quad \Gamma_{\perp}(q) = (A + Cq^2) / \tau_0. \quad (54)$$

For small q , we have $\Gamma_{\perp}(q) \ll \Gamma_{\parallel}(q)$, so $\hat{\mathbf{p}}_{\perp}$ relaxes slowly on the time scale of τ_D with

$$\tau_D = \lim_{q \rightarrow 0} \Gamma_{\perp}(q)^{-1} = \tau_0 / A. \quad (55)$$

Here, τ_D is the Debye relaxation time and will be estimated for BaTiO₃ (see Eqs.(59) and (71)). On the other hand, \mathbf{u} obeys the dynamic elasticity equation,

$$\rho \frac{\partial^2}{\partial t^2} u_\alpha = - \left(\frac{\delta \mathcal{F}}{\delta u_\alpha} \right)_{\mathbf{p}} = \sum_{\beta} \nabla_{\beta} \sigma_{\alpha\beta} - \sum_{\beta} \nabla_{\beta} \Pi_{\alpha\beta}^{\text{s}}, \quad (56)$$

where $\sigma_{\alpha\beta}$ and $\Pi_{\alpha\beta}^s$ are given in Eqs.(9) and (12) and the last term in Eq.(20) is neglected. The dissipatin of \mathbf{u} arises from the thermal fluctuations of the ES force density $-\sum_{\beta}\nabla_{\beta}\Pi_{\alpha\beta}^s$.

To describe the thermal fluctuations of \mathbf{p} , we should treat Eq.(53) as a Langevin equation to by adding a random noise term related to the kinetic coefficient $1/\tau_0$ [18, 91]. Then, we can calculate the polarization time-correlation function $\hat{G}_{\alpha\beta}(\mathbf{q}, t)$, which is divided into the longitudinal and transverse parts as

$$\begin{aligned}\hat{G}_{\alpha\beta}(\mathbf{q}, t) &= \langle \hat{p}_{\alpha}(\mathbf{q}, t)\hat{p}_{\beta}(\mathbf{q}, 0)^* \rangle / V k_B T = \hat{G}_{\parallel}(\mathbf{q}, t)\hat{q}_{\alpha}\hat{q}_{\beta} + \hat{G}_{\perp}(\mathbf{q}, t)(\delta_{\alpha\beta} - \hat{q}_{\alpha}\hat{q}_{\beta}), \\ \hat{G}_{\parallel}(\mathbf{q}, t) &= e^{-t\Gamma_{\parallel}(q)} / (A + 4\pi + Cq^2), \quad \hat{G}_{\perp}(\mathbf{q}, t) = e^{-t\Gamma_{\perp}(q)} / (A + Cq^2),\end{aligned}\quad (57)$$

From Eq.(54) $\hat{G}_{\perp}(\mathbf{q}, t)$ decays slowly and $\hat{G}_{\parallel}(\mathbf{q}, t)$ rapidly at small q . We neglect the third order ES coupling in Eqs.(53)-(57). For highly polar fluids, Ladanyi and Skaf [97] confirmed Eq.(57) at small q using molecular dynamics simulation.

We also present the dynamic equation for the sample average $\bar{p}_z(t) = \int d\mathbf{r} p_z(\mathbf{r}, t) / V$ of the z component p_z . In the geometry of parallel metal plates, it reads

$$\frac{\partial}{\partial t}\bar{p}_z = -\frac{1}{\tau_D}\bar{p}_z + \frac{1}{\tau_0}E_a = -\frac{1}{\tau_D}\bar{p}_z + \frac{4\pi}{\tau_0}(\bar{\sigma}_0 - \bar{p}_z). \quad (58)$$

Here, \bar{p}_z relaxes with the rate $1/\tau_D$ at fixed $E_a = \Phi_a/H$ and with $1/\tau_D + 4\pi = (4\pi + A)/\tau_0$ at fixed $\bar{\sigma}_0 = Q_0/L^2$ from $E_a = 4\pi(\bar{\sigma}_0 - \bar{p}_z)$, where the surface potential drops are neglected. This dramatic difference of the relaxation rates of \bar{p}_z is known for polar fluids [65, 68].

We consider the thermal average $\langle \bar{p}_z(t) \rangle$ induced by a small oscillatory $E_a = \Phi_a/H$ along the z axis, which depend on t as $e^{i\omega t}$ in the complex number representation. Then, for large systems, Eq.(58) gives the frequency-dependent dielectric constant [98–101],

$$\epsilon^*(\omega) = 4\pi\langle \bar{p}_z(t) \rangle / E_a = \epsilon / (1 + i\omega\tau_D). \quad (59)$$

Thus, τ_D in Eq.(55) is the Debye relaxation time. Furthermore, for thin films with thickness H , Eq.(21) is generalized to give the effective frequency-dependent dielectric constant [68],

$$\epsilon_{\text{eff}}^*(\omega) = [1/\epsilon^*(\omega) + 2\ell_s/H]^{-1} = \epsilon_{\text{eff}} / (1 + i\omega\tau_D'), \quad (60)$$

where the relaxation time is decreased as $\tau_D' = \tau_D / (1 + 2\ell_s/H)$ due to finite H .

4.2. Time-correlation of electrostrictive displacement

We first consider the ES displacement $\hat{m}_{\alpha}(\mathbf{q}, t)$ in Eq.(31), whose time-evolution is governed

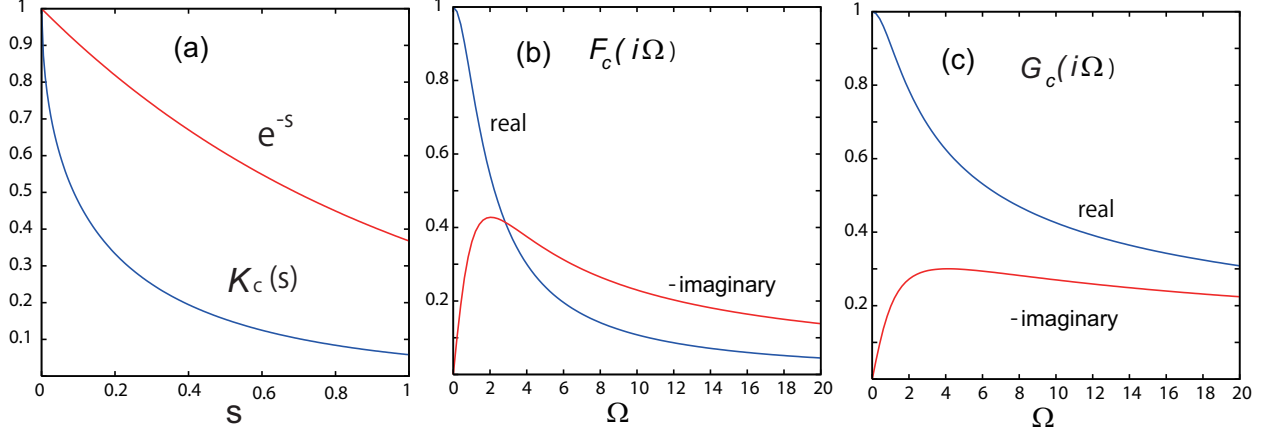


FIG. 2: (a) Scaling function $K_c(s)$ (blue line) in Eq.(68) with $s = 2t/\tau_D$, which has a cusp at $s = 0$ and decays faster than e^{-s} (red line). (b) Real part and imaginary parts of the scaling function $F_c(i\Omega)$ in Eq.(69) with $\Omega = \omega\tau_D/2$, which decay slowly for $\Omega \gtrsim 4$. (c) Real part and imaginary parts of the scaling function $G_c(i\Omega)$ in Eq.(77), which also decay slowly for $\Omega \gtrsim 4$.

by Eq.(53). The time-correlation function of $\hat{\mathbf{m}}(\mathbf{q}, t)$ and its FL transform are written as

$$\hat{R}_{\alpha\beta}(\mathbf{q}, t) = \langle \hat{m}_\alpha(\mathbf{q}, t) \hat{m}_\beta(\mathbf{q}, 0)^* \rangle / V = \frac{k_B T}{q^2} \sum_{\gamma, \nu} Z^{\alpha\gamma} Z^{\beta\nu} \hat{\Psi}_{\gamma\nu}(\hat{\mathbf{q}}, t). \quad (61)$$

$$R_{\alpha\beta}^*(\mathbf{q}, \omega) = \int_0^\infty dt e^{-i\omega t} \hat{R}_{\alpha\beta}(\mathbf{q}, t) = \frac{k_B T}{q^2} \sum_{\gamma, \nu} Z^{\alpha\gamma} Z^{\beta\nu} \zeta_{\gamma\nu}^*(\omega). \quad (62)$$

Here, $\hat{\Psi}_{\alpha\beta}(\hat{\mathbf{q}}, t)$ is the stress time-correlation function and $\zeta_{\alpha\beta}^*(\hat{\mathbf{q}}, \omega)$ is its FL transform,

$$\hat{\Psi}_{\alpha\beta}(\hat{\mathbf{q}}, t) = \frac{1}{k_B T} \sum_{\gamma, \nu} \hat{q}_\gamma \hat{q}_\nu \int d\mathbf{r} \langle \delta\Pi_{\alpha\gamma}^s(\mathbf{r}, t) \delta\Pi_{\beta\nu}^s(\mathbf{0}, 0) \rangle, \quad (63)$$

$$\zeta_{\alpha\beta}^*(\hat{\mathbf{q}}, \omega) = \int_0^\infty dt e^{-i\omega t} \hat{\Psi}_{\alpha\beta}(\hat{\mathbf{q}}, t), \quad (64)$$

where $\delta\Pi_{\alpha\gamma}^s = \Pi_{\alpha\gamma}^s - \langle \Pi_{\alpha\gamma}^s \rangle$. From Eq.(37) we have $\hat{\Psi}_{\alpha\beta}(\hat{\mathbf{q}}, 0) = \Psi_{\alpha\beta}(\hat{\mathbf{q}})$ and $\zeta_{\alpha\beta}^*(\hat{\mathbf{q}}, \omega) \rightarrow \Psi_{\alpha\beta}(\hat{\mathbf{q}})/i\omega$ as $\omega \rightarrow \infty$. We call $\zeta_{\alpha\beta}^*(\omega)$ the frequency-dependent viscosity in solids [69, 102]. Though $Z^{\alpha\beta}(\hat{\mathbf{q}})$, $\Psi_{\alpha\beta}(\hat{\mathbf{q}})$, and $\zeta_{\alpha\beta}^*(\hat{\mathbf{q}}, \omega)$ depend on $\hat{\mathbf{q}}$ even in the limit $q\xi \ll 1$, their $\hat{\mathbf{q}}$ -dependence will be suppressed in many relations to follow.

In Appendix C, we shall see that the above correlation functions depend on t and ω as

$$\hat{\Psi}_{\alpha\beta}(\hat{\mathbf{q}}, t) = \Psi_{\alpha\beta}(\hat{\mathbf{q}}) K_c(2t/\tau_D), \quad \zeta_{\alpha\beta}^*(\hat{\mathbf{q}}, \omega) = \Psi_{\alpha\beta}(\hat{\mathbf{q}}) F_c(i\Omega) \tau_D / 8, \quad (65)$$

$$\hat{R}_{\alpha\beta}(\hat{\mathbf{q}}, t) = R_{\alpha\beta}(\hat{\mathbf{q}}) K_c(2t/\tau_D), \quad R_{\alpha\beta}^*(\hat{\mathbf{q}}, \omega) = R_{\alpha\beta}(\hat{\mathbf{q}}) F_c(i\Omega) \tau_D / 8, \quad (66)$$

where the static correlations $R_{\alpha\beta}(\hat{\mathbf{q}})$ in Eq.(38) and $\Psi_{\alpha\beta}(\hat{\mathbf{q}})$ in Eqs.(39) and (40) grow as $A^{-1/2}$. Here, t is scaled by $\tau_D/2$ and ω by $2/\tau_D$. Thus, we introduce the scaled frequency,

$$\Omega = \omega\tau_D/2 = \omega\tau_0/2A. \quad (67)$$

The scaling functions $K_c(s)$ and $F_c(x)$ in Eqs.(65) and (66) are defined by

$$K_c(s) = \frac{4}{\pi} \int_0^\infty dx \frac{x^2 \exp[-s - sx^2]}{(1+x^2)^2} = \sqrt{8/\pi} D_{-3}(\sqrt{2s}), \quad (68)$$

$$F_c(x) = 4 \int_0^\infty ds e^{-xs} K_c(s) = \frac{8}{x^2} \left[1 + \frac{x}{2} - \sqrt{1+x} \right], \quad (69)$$

where $K_c(s)$ is proportional to $\int d\mathbf{q} \hat{G}_\perp(q, t)^2$, $D_{-3}(x)$ is the Weber function, and the Laplace transform of $K_c(s)$ is $F_c(x)/4$. In Fig.2, we plot $K_c(s)$ and $F_c(i\Omega)$. Here, $K_c(s) \cong 1 - 4\sqrt{s/\pi}$ for $0 < s \ll 1$ and $K_c(s) \cong \sqrt{\pi}e^{-s}/s^{3/2}$ for $s \gg 1$, while $F_c(i\Omega) \cong 1 - i\Omega/2$ for $\Omega \ll 1$ and $F_c(i\Omega) \cong 4/i\Omega - 8/(i\Omega)^{3/2}$ for $\Omega \gg 1$. The $K_c(s)$ has a cusp at $s \cong 0$ and decays faster than e^{-s} for $s \gtrsim 1$. Thus, $\zeta_{\alpha\beta}^* \sim A^{-3/2}$ for $\Omega \ll 1$ and $i\omega\zeta_{\alpha\beta}^* \sim 1 - (1-i)\sqrt{2/\Omega}$ for $\Omega \gg 1$.

The time-correlation function $\hat{R}_{\alpha\beta}(\hat{\mathbf{q}}, t) (\propto K_c(2t/\tau_D))$ decays sharply as a function of t/τ_D , while $R_{\alpha\beta}^*(\hat{\mathbf{q}}, \omega)$ has a peak at $\omega = 0$ with a height $\propto A^{-3/2}$ and a width $\propto A$. The singularity of $R_{\alpha\beta}^*(\hat{\mathbf{q}}, \omega)$ is described by the following function of ω and A ,

$$F^{\text{R}}(\omega, A) = A^{-3/2} \text{Re}[F_c(i\Omega)] = 16 \left[\left(\sqrt{4A^2 + \omega^2\tau_0^2} + 2A \right)^{1/2} - 2A^{1/2} \right] / \omega^2\tau_0^2. \quad (70)$$

which is equal to $A^{-3/2}$ at $\omega = 0$ and $A^{-3/2}/2$ at $\omega \cong 4/\tau_D$. It decays as $16/(\omega\tau_0)^{3/2}$ for $\Omega \gg 1$, which is independent of A . In Fig.3a, $F^{\text{R}}(\omega, A)$ is displayed, which is much enlarged for $A \sim 10^{-3}$ and $\omega \lesssim 4/\tau_D$. Hereafter, $\text{Re}[\dots]$ and $\text{Im}[\dots]$ denote taking the real part and the imaginary part of complex numbers, respectively.

The real part of $R_{\alpha\beta}^*(\hat{\mathbf{q}}, \omega)$ in Eq.(66) is the Fourier transform of $\hat{R}_{\alpha\beta}(\hat{\mathbf{q}}, t)$ divided by 2 and is proportional to $F^{\text{R}}(\omega, A)$ in Fig.3a. Thus, it exhibits the characteristic feature of the central peak observed in cubic BaTiO₃ [43, 53, 54]. In the light scattering experiment by *Ko et al.* [54], the central peak extended over a broad frequency range and its *full width at half maximum* was given by $1037(T/T_0 - 1)$ GHz = $6.5(T/T_0 - 1)$ /ps. Their finding enables us to determine τ_0 in τ_D . That is, since $\text{Re}[F_c(\Omega)]$ decays to 0.5 at $\Omega = \omega\tau_D/2 \cong 2$ in Fig.2b, we can equate their width to $4/\tau_D$ to obtain

$$\tau_D \cong 0.62/(T/T_0 - 1) \text{ (ps)} \cong 1.1 \times 10^{-2} A^{-1} \text{ (ps)}, \quad (71)$$

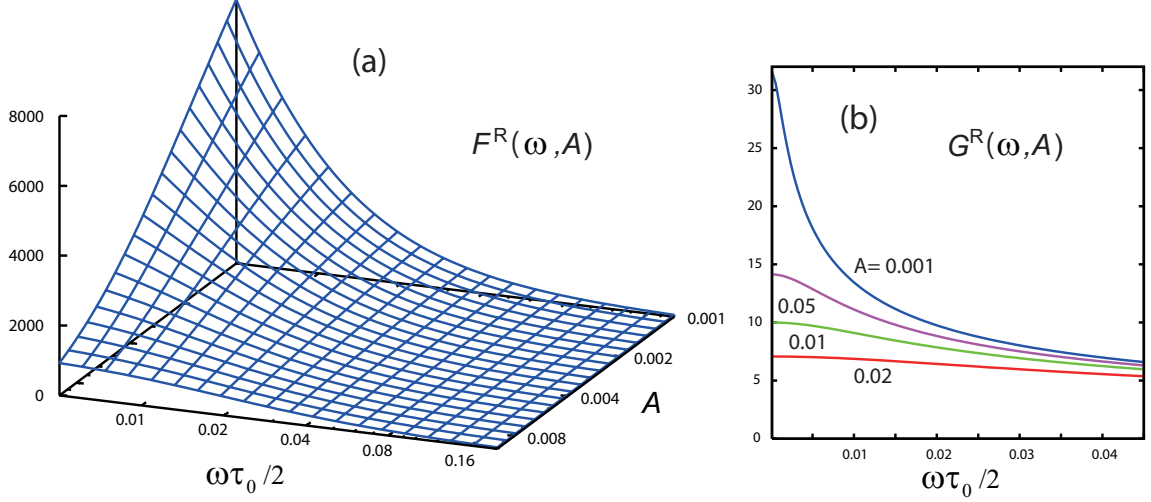


FIG. 3: (a) $F^R(\omega, A)$ in Eq.(70) as a function of $\omega\tau_0/2$ and A , which represents the near-critical strong growth of the central peak and the sound adsorption (see Eqs.(85) and (89)). (b) $G^R(\omega, A)$ in Eq.(86) vs $\omega\tau_0/2$ for three values of A , which gives the near-critical mild growth of the longitudinal sound velocity v_{11} along [001] in Eq.(84).

where we use a_1 in Eq.(6a). Thus, $\tau_0 \cong 1.1 \times 10^{-2}$ ps. However, if we use a_1 in Eq.(6b), we have $\tau_0 \cong 2.2 \times 10^{-2}$ ps.

We make remarks on other experiments on cubic BaTiO₃. (i) In their neutron scattering experiment, Yamada *et al.* [43] observed central peaks in the range $|\omega| \lesssim 1/\text{ps}$ ($= 0.6$ meV) at $T = 410$ K, which is consistent with the result by Ko *et al.* [54] for $T/T_c - 1 \sim 0.1$. (ii) In their hyper-Raman scattering experiment, Vogt *et al.* [100] obtained $\tau_D = 0.95$ ps at $T = 446$ K, which is about one-third of the value indicated by Eq.(71), however.

4.3. Time-correlation of acoustic displacement and elastic moduli

Next, we consider the dynamics of the acoustic displacement $\hat{w}_\alpha(\mathbf{q}, t)$ in Eq.(31). The time-correlation of $\hat{w}_\alpha(\mathbf{q}, t)$ and its FL transform are written as

$$\hat{S}_{\alpha\beta}(\mathbf{q}, t) = \langle \hat{w}_\alpha(\mathbf{q}, t) \hat{w}_\beta(\mathbf{q}, 0)^* \rangle / V, \quad S_{\alpha\beta}^*(\mathbf{q}, \omega) = \int_0^\infty dt e^{-i\omega t} \hat{S}_{\alpha\beta}(\mathbf{q}, t), \quad (72)$$

where $\hat{S}_{\alpha\beta}(\mathbf{q}, 0) = k_B T \rho Z^{\alpha\beta} / q^2$ and $S_{\alpha\beta}^*(\mathbf{q}, \omega) \rightarrow k_B T \rho Z^{\alpha\beta} / i\omega q^2$ as $\omega \rightarrow \infty$. In this paper, the total displacement time-correlation, written as $\hat{U}_{\alpha\beta}(\mathbf{q}, t)$, is approximated as the sum of

the ES part $\hat{R}_{\alpha\beta}(\mathbf{q}, t)$ and the acoustic part $\hat{S}_{\alpha\beta}(\mathbf{q}, t)$ as

$$\hat{U}_{\alpha\beta}(\mathbf{q}, t) = \langle \hat{u}_\alpha(\mathbf{q}, t) \hat{u}_\beta(\mathbf{q}, 0)^* \rangle / V = \hat{S}_{\alpha\beta}(\mathbf{q}, t) + \hat{R}_{\alpha\beta}(\mathbf{q}, t), \quad (73)$$

$$U_{\alpha\beta}^*(\mathbf{q}, \omega) = \int_0^\infty dt e^{-i\omega t} \hat{U}_{\alpha\beta}(\mathbf{q}, t) = S_{\alpha\beta}^*(\mathbf{q}, \omega) + R_{\alpha\beta}^*(\mathbf{q}, \omega). \quad (74)$$

Here, we neglect the cross time-correlation $\langle \hat{m}_\alpha(\mathbf{q}, t) \hat{w}_\beta(\mathbf{q}, 0)^* \rangle = \langle \hat{w}_\alpha(\mathbf{q}, t) \hat{m}_\beta(\mathbf{q}, 0)^* \rangle$. This is justified if the time-evolution of \mathbf{p} is not affected by \mathbf{u} via the ES coupling. It is indeed assumed in Eqs.(53) and (57).

In the linear response scheme [72, 93, 103, 104], $S_{\alpha\beta}^*(\mathbf{q}, \omega)$ obeys the 3×3 matrix equation,

$$\sum_\gamma \left[-\rho\omega^2 \delta_{\alpha\gamma} + q^2 Z_{\alpha\gamma}^*(\hat{\mathbf{q}}, \omega) \right] S_{\gamma\beta}^*(\mathbf{q}, \omega) = i\omega k_B T \rho Z^{\alpha\beta} / q^2, \quad (75)$$

where $\{Z_{\alpha\gamma}^*(\hat{\mathbf{q}}, \omega)\}$ is the frequency-dependent Christoffel matrix. written as

$$\begin{aligned} Z_{\alpha\beta}^*(\hat{\mathbf{q}}, \omega) &= Z_{\alpha\beta} - \Psi_{\alpha\beta} + i\omega \zeta_{\alpha\beta}^*(\omega) = Z_{\alpha\beta} + \int_0^\infty dt e^{-i\omega t} \frac{d}{dt} \hat{\Psi}_{\alpha\beta}(\hat{\mathbf{q}}, t) \\ &= Z_{\alpha\beta} - \Psi_{\alpha\beta} G_c(i\Omega). \end{aligned} \quad (76)$$

Here, $\zeta_{\alpha\beta}^*(\omega)$ is given in Eq.(64). In the second line we define the function $G_c(i\Omega)$ by

$$\begin{aligned} G_c(i\Omega) &= 1 - i\Omega F_c(i\Omega)/4 = 2(\sqrt{1+i\Omega} - 1)/i\Omega \\ &= (2\sqrt{1+\Omega^2} - 2)^{1/2}/\Omega - i \left[(2\sqrt{1+\Omega^2} + 2)^{1/2} - 2 \right] / \Omega, \end{aligned} \quad (77)$$

where the real and imaginary parts are written separately as displayed in Fig.2c. Here, $G_c(i\Omega) \cong 1 - i\Omega/4 - 5\Omega^2/16$ for $\Omega \ll 1$ and $G_c(i\Omega) \cong 2/\sqrt{i\Omega} = (1-i)\sqrt{2/\Omega}$ for $\Omega \gg 1$. We can see $\text{Im}(G_c) < 0$ leading to positive entropy production. The sound dispersion relations with damping are given by vanishing of the determinant of the matrix $-\rho\omega^2 \delta_{\alpha\beta} + q^2 Z_{\alpha\beta}^*$.

As a generalization of Eq.(48), we use Eqs.(26), (27), (40), and (76) to obtain the renormalized frequency-dependent elastic moduli,

$$C_{ij}^*(\omega) = c_{ij} - M_{ij} I_e A^{-1/2} G_c(i\Omega) = C_{ij} + M_{ij} I_e A^{-1/2} i\Omega F_c(i\Omega)/4. \quad (78)$$

Writing $C_{ij}^*(\omega)$ as C_{ij}^* , we find the frequency-dependent Christoffel matrix,

$$Z_{\alpha\beta}^*(\hat{\mathbf{q}}, \omega) = (C_{44}^* + (C_{11}^* - C_{12}^* - 2C_{44}^*) \hat{q}_\alpha^2) \delta_{\alpha\beta} + (C_{12}^* + C_{44}^*) \hat{q}_\alpha \hat{q}_\beta, \quad (79)$$

where c_{ij} in Z_{ij} in Eq.(26) are replaced by C_{ij}^* . From Eq.(78) $C_{ij}^*(\omega)$ behave as

$$C_{ij}^*(\omega) \cong c_{ij} - M_{ij} I_e A^{-1/2} (1 - i\omega\tau_D/8) \quad (\omega\tau_D \ll 1) \quad (80a)$$

$$\cong c_{ij} - 2M_{ij} I_e (1-i)(\omega\tau_0)^{-1/2} \quad (\omega\tau_D \gg 1), \quad (80b)$$

where $C_{ij}^*(\omega)$ are independent of A for $\omega\tau_D \gg 1$. In particular, if $\hat{\mathbf{q}}$ is along [001], we have $\hat{q}_\alpha^2 = \delta_{\alpha z}$ and $\hat{q}_\alpha \hat{q}_\gamma = \delta_{\alpha z} \delta_{\gamma z}$, so Eq.(75) is readily solved to give

$$S_{\alpha\beta}(\mathbf{q}, \omega) = k_B T \frac{i\omega\rho}{q^2} \left[\frac{\delta_{\alpha z} \delta_{\beta z}}{c_{11}(-\rho\omega^2 + q^2 C_{11}^*)} + \frac{\delta_{\alpha\beta} - \delta_{\alpha z} \delta_{\beta z}}{c_{44}(-\rho\omega^2 + q^2 C_{44}^*)} \right] \quad (\hat{\mathbf{q}} \parallel [001]). \quad (81)$$

We will solve Eq.(75) for general $\hat{\mathbf{q}}$ in Appendix D. .

From the cubic symmetry we find the correlation-function expressions of $C_{ij}^*(\omega)$ as

$$\begin{aligned} C_{11}^*(\omega) &= c_{11} + \mathcal{G}_{zz}^{zz}(\omega), & C_{44}^*(\omega) &= c_{44} + \mathcal{G}_{zx}^{zx}(\omega), \\ C_{12}^*(\omega) &= c_{12} + \frac{1}{6} \sum_{\alpha \neq \beta} \mathcal{G}_{\alpha\alpha}^{\beta\beta}(\omega). \end{aligned} \quad (82)$$

Here, we define the following correlation functions,

$$\mathcal{G}_{\alpha\gamma}^{\beta\nu}(\omega) = \frac{1}{k_B T} \int_0^\infty dt e^{-i\omega t} \frac{d}{dt} \int d\mathbf{r} \langle \delta\Pi_{\alpha\gamma}^s(\mathbf{r}, t) \delta\Pi_{\beta\nu}^s(\mathbf{0}, 0) \rangle, \quad (83)$$

which will be calculated in Appendix C in the mean-field theory. We note that $\int d\mathbf{r} \langle \delta\Pi_{\alpha\gamma}^s(\mathbf{r}, t) \delta\Pi_{\beta\nu}^s(\mathbf{0}, 0) \rangle / k_B T$ are the response functions in Kubo's theory [105].

4.4. Acoustic anomaly due to electrostrictive coupling

As can be known from Eq.(81), the displacement of the longitudinal sound along [001] is expressed as $\text{const.} \exp[i\omega t - iq^* z]$ with $q^* = \omega(\rho/C_{11}^*)^{1/2}$ in the complex number representation. For this acoustic mode, the velocity $v_{11} = \text{Re}(\omega/q^*)$ and the absorption coefficient $\alpha_{11}^L = -\text{Im}(q^*)$ are expressed in terms of $G_c(i\Omega)$ in Eq.(77) as

$$\frac{v_{11}}{v_{11}^0} = 1 - \frac{\Delta C_{11}}{2c_{11}} \text{Re}[G_c(i\Omega)] = 1 - 2.2 \times 10^{-3} G^R(\omega, A), \quad (84)$$

$$\frac{v_{11}^0}{\omega} \alpha_{11}^L = -\frac{\Delta C_{11}}{2c_{11}} \text{Im}[G_c(i\Omega)] = 2.7 \times 10^{-4} \omega\tau_0 F^R(\omega, A). \quad (85)$$

Here, $v_{11}^0 = \sqrt{c_{11}/\rho}$ is the unrenormalized sound velocity and the experimental $\Delta C_{11}/c_{11}$ in the limit $\omega \rightarrow 0$ is given in Eq.(49). In Eq.(84) we define the function,

$$G^R(\omega, A) = A^{-1/2} \text{Re}[G_c(i\Omega)] = 2 \left(\sqrt{4A^2 + \omega^2 \tau_0^2} - 2A \right)^{1/2} / \omega\tau_0, \quad (86)$$

which is plotted in Fig.3b. The growth of $G^R(\omega, A)$ at small A is much milder than that of $F^R(\omega, A)$ in Fig.3a. Thus, $1 - v_{11}/v_{11}^0 \propto A^{-1/2}$ and $\alpha_{11}^L \propto \omega^2 A^{-3/2}$ for $\Omega \ll 1$. However, for $\Omega \gg 1$, they are independent of A as

$$1 - v_{11}/v_{11}^0 \cong (v_{11}^0/\omega) \alpha_{11}^L \cong 0.43 \times 10^{-2} (\omega\tau_0)^{-1/2}. \quad (87)$$

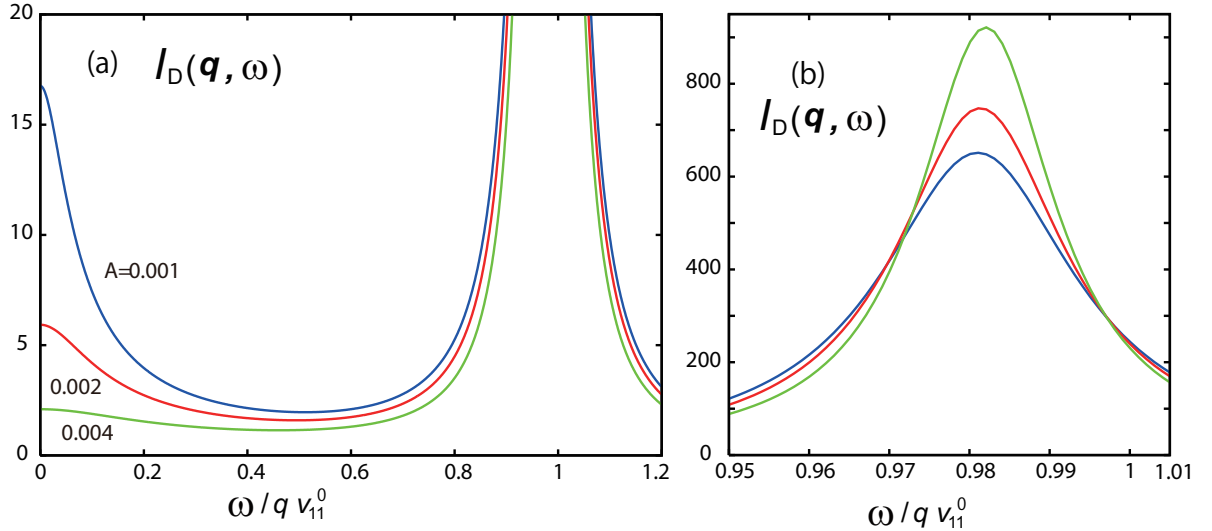


FIG. 4: Normalized dynamic structure factor $(c_{11}/k_B T \tau_0) I_D(q, \omega)$ in Eq.(89) vs scaled frequency ω/qv_{11}^0 along [001] for $q = 0.08 \text{ \AA}$ and $v_{11}^0 = 5.87 \times 10^5 \text{ cm/s}$. (a) The central peak is shown for $A = 0.001, 0.002,$ and 0.004 in the range $0 < \omega/qv_{11}^0 < 1.2$, where $qv_{11}^0 \tau_D = 0.052/A \gg 1$ for these A . (b) The acoustic peak of $(c_{11}/k_B T \tau_0) I_D(q, \omega)$ is shown in the range $0.95 < \omega/qv_{11}^0 < 1.01$.

The above crossover occurs at very small ω for $A \ll 1$ (see Fig.3b),

We comment on previous theories on the critical sound absorption, where the stress tensor contains slowly relaxing terms quadratic in the order parameter. (i) Levanyuk [35] assumed the ES coupling of the isotropic form $\propto |\mathbf{p}|^2 \nabla \cdot \mathbf{u}$ (in the case of $g_{11} - g_{12} = g_{44} = 0$ in our Eq.(12)). He calculated the four-body time-correlation (FBTC) of \mathbf{p} . Indeed, in his Eqs.(19) and (20), he calculated $G_c(i\Omega)$ in our Eq.(77). (ii) Minaeva *et al.* [37, 38] assumed the ES coupling for uniaxial TGS. They calculated FBTC of the order parameter p_y using Krivoglaz's theory [25] to find a critical growth of the absorption coefficient ($\propto A^{-1}$) in the low frequency limit. (iii) Dvořák [36] assumed the general form of the ES coupling for BaTiO₃ and calculated FBTC, but he assumed its exponential relaxation not using $K_c(s)$ in our Eq.(68). (iv) The sound attenuation was studied for ferromagnets in the asymptotic critical region by Kawasaki [106] and by Laramore and Kadanoff [107]. They calculated FBTC of the magnetization in the low frequency limit in the mode-coupling theory, but they neglected the anisotropy in the crystal elasticity. (v) Analogously to $\zeta_{\alpha\beta}^*(\hat{\mathbf{q}}, \omega)$ in Eqs.(64) and (65), the bulk viscosity in near-critical fluids is strongly divergent and frequency-dependent, which is given by the FL transform of FBTC of the order parameter (the mass density or

the composition) [18, 104, 108].

4.5. Density time-correlation and dynamic structure factor

We consider the FL transform of the density time-correlation in the limit $q \rightarrow 0$:

$$\begin{aligned} I_D^*(\mathbf{q}, \omega) &= \int_0^\infty dt e^{-i\omega t} \langle \hat{\rho}(\mathbf{q}, t) \hat{\rho}(\mathbf{q}, 0)^* \rangle / V \rho^2 = \sum_{\alpha, \beta} q_\alpha q_\beta U_{\alpha\beta}^*(\mathbf{q}, \omega) \\ &= \sum_{\alpha, \beta} q_\alpha q_\beta S_{\alpha\beta}^*(\hat{\mathbf{q}}, \omega) + \frac{k_B T I_e \tau_0}{8(c_{12} + c_{44})^2} D(\hat{\mathbf{q}}) A^{-3/2} F_c(i\Omega), \end{aligned} \quad (88)$$

which tends to $I_D(\mathbf{q})/i\omega$ as $\omega \rightarrow \infty$ from Eq.(41). The acoustic part $\sum_{\alpha, \beta} q_\alpha q_\beta S_{\alpha\beta}^*$ for general $\hat{\mathbf{q}}$ will be calculated in Appendix D. In the ES part, $D(\hat{\mathbf{q}})$ is given in Eq.(43) and Fig.1. The real part $I_D(\mathbf{q}, \omega) = \text{Re}[I_D^*(\mathbf{q}, \omega)]$ is called the dynamic structure factor. It exhibits the Brillouin and central peaks, whose ω -integrals in the range $\omega > 0$ are the two terms in $I_D(\mathbf{q})$ in Eq.(42) multiplied by π . Here, using Eq.(81), we calculate $I_D(\mathbf{q}, \omega)$ for \mathbf{q} along [001]:

$$\frac{c_{11}}{k_B T \tau_0} I_D(\mathbf{q}, \omega) = \text{Re} \left(\frac{-\rho i \omega / \tau_0}{\rho \omega^2 - q^2 C_{11}^*} \right) + \frac{c_{11} I_e D[001]}{8(c_{12} + c_{44})^2} F^{\text{R}}(\omega, A) \quad (\mathbf{q} \parallel [001]), \quad (89)$$

where $D[001] = 2.8$ in Fig.1, $F^{\text{R}}(\omega, A)$ is given in Eq.(70), and the coefficient in front of $F^{\text{R}}(\omega, A)$ is estimated to be 5.4×10^{-3} from Table 1 and Eq.(71). The height and width of the acoustic part are $1/(2v_{11}^0 \alpha_{11}^{\text{L}} \tau_0)$ and $v_{11}^0 \alpha_{11}^{\text{L}}$, respectively, in terms of α_{11}^{L} in Eq.(85), while those of the ES part are $5.4 \times 10^{-3} A^{-3/2}$ and $4/\tau_D$, respectively.

In Fig.4, we plot $I_D(\mathbf{q}, \omega)$ along [001] vs ω/qv_{11}^0 , where $q = 0.08/\text{\AA}$, $v_{11}^0 = 5.87 \times 10^5$ cm/s, and $qv_{11}^0 = 4.7/\text{ps}$ (= 750 GHz = 2.9 meV). This q value was used in the neutron scattering experiment by Yamada *et al* [43]. For the three curves in Fig.4, we set $A = 0.001, 0.002,$ and 0.004 using $a_1 = 1.8 \times 10^{-2}$ in Eq.(6a), for which $qv_{11}^0 \tau_D = 52, 26,$ and $13,$ respectively. Thus, in Fig.4, the acoustic frequency qv_{11} exceeds the central peak width $4/\tau_D$. We also notice that v_{11} and α_{11}^{L} are insensitive to A from Eq.(87). We can also see that the peak height of the central peak is much lower than that of the acoustic peak for $T > T_c$. From Eqs.(85) and (89) the ratio of these heights is calculated as

$$\frac{\text{central peak height}}{\text{acoustic peak height}} = 4.8 \times 10^{-6} \left[\left(\sqrt{4 + (qv_{11}^0 \tau_0)^2 / A^2} + 2 \right)^{1/2} - 2 \right] / A, \quad (90)$$

where grows as $A \rightarrow 0$ but the coefficient is very small. For $A \ll qv_{11}^0 \tau_0$, the above ratio becomes $4.8 \times 10^{-6} \sqrt{qv_{11}^0 \tau_0} A^{-3/2}$, which is the case in Fig.4.

We make remarks. (i) In the neutron scattering experiment by Yamada *et al.* the central peak decreased with further increasing q to $0.12/\text{\AA}$ and $0.16/\text{\AA}$ in their Fig.7. This large- q

behavior is beyond the scope of this paper since the limit $q \rightarrow 0$ is taken in our theory. (ii) Along [001], Ko *et al.* [54] set $q \cong 4 \times 10^{-3}/\text{\AA}$ in measuring the Brillouin shift (in their Fig.1) and $q \cong 4 \times 10^{-2}/\text{\AA}$ in measuring the central peak in their Fig.4, where the acoustic frequency is at most comparable to the central peak width.

5. Summary and remarks

We have presented a Ginzburg-Landau theory of the central peak and the acoustic anomaly in paraelectric BaTiO₃, which originate from the electrostrictive (ES) coupling between the polarization \mathbf{p} and the displacement \mathbf{u} . We have used the mean-field theory, which is justified by the Ginzburg criterion in Sec.3.1. Our main results are summarized as follows.

In Sec.2, we have presented the free energy functional \mathcal{F} , where the ES stress tensor $\Pi_{\alpha\beta}^s$ in Eqs.(11) and (12) is a key quantity. The total stress tensor has been given in Eq.(16).

In Sec.3, the static correlations of \mathbf{p} and \mathbf{u} have been calculated. In Sec.3.2, those of the longitudinal and transverse Fourier components of \mathbf{p} have been given in Eq.(28). In Sec.3.3, \mathbf{u} has been divided into the ES part \mathbf{m} and the acoustic part \mathbf{w} in Eq.(31) with their correlations in Eq.(37). The ES correlation $R_{\alpha\beta}(\mathbf{q})$ grows as $A^{-1/2}$ in the limit $q \rightarrow 0$ and is related to the ES coefficients g_{ij} in Eqs.(38)-(40). In Sec.3.4, we have also examined the density correlation $I_D(\mathbf{q})$ in Eq.(42), whose ES part is proportional to the anisotropy factor $D(\hat{\mathbf{q}})$ in Fig.1. In Sec.3.5, we have calculated the renormalized static elastic moduli C_{ij} in Eq.(48). We have then determined the coefficient C in the gradient free energy in Eq.(50) using the data by Kashida *et al.* [40]. In Sec.3.6, we have obtained the free energy contribution $\Delta\mathcal{F}_{\text{inh}}^{\text{po}}$ from the inhomogeneous displacement fluctuations in Eq.(51).

In Sec.4-1, starting with the dynamic equations for \mathbf{p} , we have calculated the time-correlation function of \mathbf{p} in Eq.(57). The effective dielectric constant for films has been given in Eqs.(59) and (60). In Sec.4-2, we have examined the time-correlations of the ES displacement, $\hat{R}_{\alpha\beta}(\mathbf{q}, t)$ and $R_{\alpha\beta}^*(\mathbf{q}, \omega)$, in Eqs.(61) and (62) in terms of the stress time correlations in Eqs.(61) and (62). These functions involve the Debye relaxation time $\tau_D = \tau_0/A$ and depend on t and ω simply as in Eqs.(62) and (63). The ES correlation $R_{\alpha\beta}^*(\mathbf{q}, \omega)$ has the characteristic feature of the central peak. as is evident in Fig.3a. We have then determined τ_D in Eq.(68) using the data by Ko *et al.* [41]. In Sec.4-3, we have calculated the time-correlations of the acoustic displacement, $\hat{S}_{\alpha\beta}(\mathbf{q}, t)$ and $S_{\alpha\beta}^*(\mathbf{q}, \omega)$, in Eq.(69). We have then obtained the frequency-dependent elastic moduli $C_{ij}^*(\omega)$ in Eqs.(78) and (80), where the

critical part of $C_{44}^*(\omega)$ is very small. In Sec.4-4, we have examined the acoustic anomaly of the longitudinal sound along [001] in Eqs.(84)-(87). In Sec.4-5, the density time-correlation $I_D(\mathbf{q}, \omega)$ in Eq.(89) has been displayed in Fig.4 in accord with the scattering experiment by Yamada *et al.* [43].

We remark on future work. (i) We will shortly present a theory on the central peak in tetragonal uniaxial KDP, where the piezoelectric stress is given by $g_{36}p_z(\delta_{\alpha x}\delta_{\beta y} + \delta_{\alpha y}\delta_{\beta x})$ with g_{36} being a constant. (ii) We should also present a theory below T_c . (iii) Domain dynamics in various ferroelectrics is of great interest [16, 17], where an electric field can be applied. (iv) In systems with large dielectric constants, the statics and dynamics generally depend on whether the surface charge Q_0 is fixed or the potential difference Φ_a is fixed (see below Eq.(58)) [65, 66, 68]. That is, at fixed Φ_a , the space-time polarization correlations acquire nonlocal parts inversely proportional to the volume V , whose sample integral determines the overall dielectric response.

Data availability

The data that supports the findings of this study are available within the article.

Appendix A: Global mechanical equilibrium in unclamped samples

In unclamped samples, homogeneous strains can be induced by overall polarization. Thus, we write the sample averages of $\epsilon_{\alpha\beta}$, $\sigma_{\alpha\beta}$, $\Pi_{\alpha\beta}^s$, and $\epsilon_{\alpha\beta}^s$ as $\overline{\epsilon_{\alpha\beta}}$, $\overline{\sigma_{\alpha\beta}}$, $\overline{\Pi_{\alpha\beta}^s}$, and $\overline{\epsilon_{\alpha\beta}^s}$, respectively, with overlines. They are the Fourier components with $\mathbf{q} = \mathbf{0}$ divided by V (see Eq.(23)). For example, we can prepare a stress-free paraelectric state with $\mathbf{u} = \mathbf{p} = \mathbf{0}$ and apply a small electric field. Then, these sample averages become nonvanishing. Their contribution to $\int d\mathbf{r}(f_{\text{el}} + f_{\text{int}})$ is written as

$$\Delta\mathcal{F}_{\text{hom}}^{\text{el}} = V \sum_{\alpha,\beta} \left(\frac{1}{2} \overline{\sigma_{\alpha\beta}} \cdot \overline{\epsilon_{\alpha\beta}} - \overline{\Pi_{\alpha\beta}^s} \cdot \overline{\epsilon_{\alpha\beta}^s} \right), \quad (\text{A1})$$

which is minimized with respect to $\overline{\epsilon_{\alpha\beta}}$ in the mechanical equilibrium at given $\overline{\Pi_{\alpha\beta}^s}$. Then,

$$\overline{\epsilon_{\alpha\beta}} = \overline{\epsilon_{\alpha\beta}^s}, \quad \overline{\sigma_{\alpha\beta}} = \overline{\Pi_{\alpha\beta}^s}, \quad \Delta\mathcal{F}_{\text{hom}}^{\text{el}} = -\frac{1}{2} V \sum_{\alpha,\beta} \overline{\Pi_{\alpha\beta}^s} \cdot \overline{\epsilon_{\alpha\beta}^s}, \quad (\text{A2})$$

where the first two relations are equivalent. Using Eq.(A2) the ES coefficients Q_{ij} in Eq.(13) can be determined experimentally [27, 31, 32]. From Eqs.(12)-(14) we obtain

$$\Delta\mathcal{F}_{\text{hom}}^{\text{el}}/V = -\beta_1 \sum_{\alpha} \left(\overline{p_{\alpha}^2} - \frac{1}{3} \overline{|\mathbf{p}|^2} \right)^2 - \beta_2 (\overline{|\mathbf{p}|^2})^2 - \beta_3 \left[(\overline{p_x p_y})^2 + (\overline{p_y p_z})^2 + (\overline{p_z p_x})^2 \right]. \quad (\text{A3})$$

The coefficients β_1 , β_2 , and β_3 are positive and are given by

$$\beta_1 = (g_{11} - g_{12})^2/[2(c_{11} - c_{12})], \quad \beta_2 = (g_{11} + 2g_{12})^2/[6(c_{11} + 2c_{12})], \quad \beta_3 = g_{44}^2/2c_{44}. \quad (\text{A4})$$

For BaTiO₃, Table 1 gives $\beta_1 = 0.030$, $\beta_2 = 0.0026$, and $\beta_3 = 0.0014$ in GPa⁻¹.

In Eq.(A3) the overlines can be removed for stress-free single crystals with homogeneous \mathbf{p} . After the homogeneous strains are removed in mechanical equilibrium in such samples, α_{11}^0 and α_{12}^0 in Eq.(3) are changed to

$$\alpha_{11} = \alpha_{11}^0 - 2\beta_1/3 - \beta_2, \quad \alpha_{12} = \alpha_{12}^0 + 2\beta_1/3 - 2\beta_2 - \beta_3, \quad (\text{A5})$$

For stress-free BaTiO₃, some authors [30, 31, 34] determined the Landau free energy for homogeneous \mathbf{p} to explain the observed successive first-order phase transitions, where $\Delta\mathcal{F}_{\text{hom}}^{\text{el}}$ in Eq.(A3) should be included in the free energy. Li *et al* [31] found $\alpha_{12} = 7.974 \times 10^8 \text{ C}^{-4} \text{ m}^6 \text{ N} = 0.010/\text{GPa} = 3.05/c_{11} > 0$ and $\alpha_{11} = -0.26\alpha_{12} < 0$, where α_{12} is one-third of β_1 in Eq.(A4). Then, Eq.(A5) gives $\alpha_{11}^0 = 0.025/\text{GPa} > 0$ and $\alpha_{12}^0 = -0.006/\text{GPa} < 0$. In BaTiO₃, the phase transitions delicately depend on the mechanical boundary condition.

We also note that the overlines in Eq.(A3) cannot be removed for inhomogeneous \mathbf{p} , particularly, in multi-domain states and in phase ordering. This aspect remains unexplored.

Appendix B: Gradient free energy for cubic solids

In the literature [15–17], the gradient free energy \mathcal{F}_g for BaTiO₃ consists of several terms, which are bilinear in $\nabla_\alpha p_\beta$ with four coefficients G_{11}, G_{12}, G_{44} , and G'_{44} . We express \mathcal{F}_g in terms of the Fourier components $\hat{p}_\alpha(\mathbf{q})$ with $\mathbf{q} \neq \mathbf{0}$ in Eq.(23) as

$$\mathcal{F}_g = \frac{1}{2V} \sum_{\mathbf{q} \neq \mathbf{0}} C \left[(1 - \gamma_{14} - \gamma_{44}) \sum_\alpha q_\alpha^2 |\hat{p}_\alpha(\mathbf{q})|^2 + \gamma_{14} |\mathbf{q} \cdot \hat{\mathbf{p}}(\mathbf{q})|^2 + \gamma_{44} q^2 |\hat{\mathbf{p}}(\mathbf{q})|^2 \right], \quad (\text{B1})$$

where C , γ_{14} , and γ_{44} are given by $C = G_{11} - G_{44}$, $C\gamma_{14} = G_{12} + G_{44} - G'_{44}$, and $G\gamma_{44} = G_{44} + G'_{44}$. Here, we do not write the surface contributions $\propto \int dx dy (p_\alpha \nabla_z p_\beta)_{z=0,H}$, which are relevant for thin films in the presence of the surface free energy [19].

In simulations, Nambu and Sagara [16] set $(\gamma_{14}, \gamma_{44}) = (1.9, 1)$ in two dimensions, while Hu and Chen [17] set $(\gamma_{14}, \gamma_{44}) = (0, 1)$ in three dimensions. For the latter choice, we obtain the isotropic form $\mathcal{F}_g = \sum_{\mathbf{q} \neq \mathbf{0}} C q^2 |\hat{\mathbf{p}}(\mathbf{q})|^2 / 2V$ adopted in this paper.

Appendix C: Correlations of electrostrictive tensor $\Pi_{\alpha\beta}^s$ at long wavelengths

In this appendix, we express the time-correlation of any space-time-dependent variables

$\mathcal{A}(\mathbf{r}, t)$ and $\mathcal{B}(\mathbf{r}, t)$ in the long wavelength limit as

$$\langle \mathcal{A} : \mathcal{B} \rangle(t) = \int d\mathbf{r} (\mathcal{A}(\mathbf{r}, t) - \langle \mathcal{A} \rangle) (\mathcal{B}(\mathbf{0}, 0) - \langle \mathcal{B} \rangle), \quad (\text{C1})$$

where the integrand is assumed to decay rapidly for large r . Using Eq.(57) we calculate the four-body time correlation of $m_{\alpha\gamma} = p_\alpha p_\beta$ and $m_{\beta\nu} = p_\beta p_\nu$ as

$$\begin{aligned} \langle m_{\alpha\gamma} : m_{\beta\nu} \rangle(t) &= ((2\pi)^{-3} \int d\mathbf{q} [G_{\alpha\beta}(\mathbf{q}, t)G_{\gamma\nu}(\mathbf{q}, t) + G_{\alpha\nu}(\mathbf{q}, t)G_{\gamma\beta}(\mathbf{q}, t)]) \\ &= [7(\delta_{\alpha\beta}\delta_{\gamma\nu} + \delta_{\alpha\nu}\delta_{\beta\gamma}) + 2\delta_{\alpha\gamma}\delta_{\beta\nu}]J_e(t), \end{aligned} \quad (\text{C2})$$

where we use the decoupling approximation and pick up the contributions proportional to $\int d\mathbf{q} \hat{G}_\perp(q, t)^2$. Using I_e in Eq.(30) and $K_c(s)$ in Eq.(68) we calculate $J_e(t)$ as

$$J_e(t) = (k_B T)^2 \int d\mathbf{q} G_\perp(q, t)^2 / 120\pi^3 = k_B T I_e A^{-1/2} K_c(2t/\tau_D) / 60. \quad (\text{C3})$$

It is convenient to introduce the following variables quadratic in \mathbf{p} :

$$\mathcal{D}_\alpha = p_\alpha^2 - |\mathbf{p}|^2/3, \quad \mathcal{E}_{\alpha\beta} = p_\alpha p_\beta - p_\alpha^2 \delta_{\alpha\beta}. \quad (\text{C4})$$

From Eq.(C2) $|\mathbf{p}|^2$, \mathcal{D}_α , and $\mathcal{E}_{\alpha\beta}$ are *orthogonal* to one another as

$$\langle \mathcal{D}_\alpha : \mathcal{E}_{\beta\nu} \rangle(t) = \langle \mathcal{D}_\alpha : |\mathbf{p}|^2 \rangle(t) = \langle \mathcal{E}_{\alpha\beta} : |\mathbf{p}|^2 \rangle(t) = 0. \quad (\text{C5})$$

Their self-correlations are given by

$$\begin{aligned} \langle |\mathbf{p}|^2 : |\mathbf{p}|^2 \rangle(t) &= 60J_e(t), \quad \langle \mathcal{D}_\alpha : \mathcal{D}_\beta \rangle(t) = 14(\delta_{\alpha\beta} - 1/3)J_e(t), \\ \langle \mathcal{E}_{\alpha\gamma} : \mathcal{E}_{\beta\nu} \rangle(t) &= 7(\delta_{\alpha\beta}\delta_{\gamma\nu} + \delta_{\alpha\nu}\delta_{\beta\gamma} - 2\delta_{\alpha\beta}\delta_{\gamma\nu}\delta_{\beta\nu})J_e(t). \end{aligned} \quad (\text{C6})$$

We then express the stress tensor $\Pi_{\alpha\beta}^s$ in Eq.(12) as

$$\Pi_{\alpha\beta}^s = (g_{11} - g_{12})\mathcal{D}_\alpha \delta_{\alpha\beta} + (g_{11} + 2g_{12})|\mathbf{p}|^2 \delta_{\alpha\beta} / 3 + g_{44}\mathcal{E}_{\alpha\beta}. \quad (\text{C7})$$

Using Eqs.(C5) and (C6) we find the time-correlations of the ES stress tensor,

$$\langle \Pi_{\alpha\gamma}^s : \Pi_{\beta\nu}^s \rangle(t) = 60J_e(t)\mathcal{T}_{\alpha\gamma}^{\beta\nu} = k_B T I_e A^{-1/2} \mathcal{T}_{\alpha\gamma}^{\beta\nu} K_c(2t/\tau_D), \quad (\text{C8})$$

$$\mathcal{G}_{\alpha\gamma}^{\beta\nu}(\omega) = I_e A^{-1/2} \mathcal{T}_{\alpha\gamma}^{\beta\nu} G_c(i\Omega), \quad (\text{C9})$$

where we define $\mathcal{G}_{\alpha\gamma}^{\beta\nu}(\omega)$ in Eq.(83), $G_c(i\Omega)$ in Eq.(77), and $\mathcal{T}_{\alpha\gamma}^{\beta\nu}$ as

$$\begin{aligned} \mathcal{T}_{\alpha\gamma}^{\beta\nu} &= \delta_{\alpha\gamma}\delta_{\beta\nu}(M_{11} + 2M_{12})/3 + (\delta_{\alpha\beta} - 1/3)\delta_{\alpha\gamma}\delta_{\beta\nu}(M_{11} - M_{12}) \\ &\quad + (\delta_{\alpha\beta}\delta_{\gamma\nu} + \delta_{\alpha\nu}\delta_{\beta\gamma} - 2\delta_{\alpha\beta}\delta_{\gamma\nu}\delta_{\beta\nu})M_{44}. \end{aligned} \quad (\text{C10})$$

From Eq.(39) we have $\Psi_{\alpha\beta}(\mathbf{q}) = I_e A^{-1/2} \sum_{\gamma,\nu} \hat{q}_\gamma \hat{q}_\nu \mathcal{T}_{\alpha\gamma}^{\beta\nu}$. We can then confirm Eqs.(40), (65), (66), and (82) from Eqs.(C8)-(C10).

Appendix D: Fourier-Laplace transform of acoustic time-correlation

To calculate $S_{\alpha\beta}^*(\mathbf{q}, \omega)$ for general $\hat{\mathbf{q}}$ from Eqs.(75) and (79), we define a_α^* , b^* , and $W_{\alpha\beta}^*$ by

$$\begin{aligned} a_\alpha^* &= -\rho\omega^2/q^2 + C_{44}^* + (C_{11}^* - C_{12}^* - 2C_{44}^*)\hat{q}_\alpha^2, \quad b^* = (C_{12}^* + C_{44}^*)\sum_\gamma \hat{q}_\gamma^2/a_\gamma^*, \\ W_{\alpha\beta}^* &= \delta_{\alpha\beta}/a_\alpha^* - (C_{12}^* + C_{44}^*)\hat{q}_\alpha\hat{q}_\beta/[a_\alpha^*a_\beta^*(1+b^*)], \end{aligned} \quad (\text{D1})$$

Here, the matrix $\{W_{\alpha\beta}^*\}$ is the inverse of $\{-\rho\omega^2\delta_{\alpha\beta}/q^2 + Z_{\alpha\beta}^*\}$. It is obtained from $Z^{\alpha\beta}$ in Eq.(32) by replacements: $a_\alpha \rightarrow a_\alpha^*$ and $b \rightarrow b^*$. Then, Eq.(75) yields

$$S_{\alpha\beta}^*(\mathbf{q}, \omega) = \frac{\rho k_B T i \omega}{q^4} \sum_\gamma W_{\alpha\gamma}^* Z^{\gamma\beta} = \frac{\rho k_B T i \omega}{a_\alpha^* a_\beta^* q^4} \left[\delta_{\alpha\beta} - \hat{q}_\alpha \hat{q}_\beta \Xi_{\alpha\beta}(\hat{\mathbf{q}}) \right], \quad (\text{D2})$$

where $\Xi_{\alpha\beta}$ is given by

$$\Xi_{\alpha\beta}(\hat{\mathbf{q}}) = \frac{C_{12}^* + C_{44}^*}{a_\beta^*(1+b^*)} + \frac{C_{12} + C_{44}}{a_\alpha(1+b)} - \frac{(C_{12}^* + C_{44}^*)(C_{12} + C_{44})}{(1+b^*)(1+b)} \sum_\gamma \frac{\hat{q}_\gamma^2}{a_\gamma^* a_\gamma}. \quad (\text{D3})$$

Using $\sum_\gamma W_{\alpha\gamma}^* \hat{q}_\gamma = \hat{q}_\alpha/a_\alpha^*(1+b^*)$ the acoustic part in Eq.(88) is expressed as

$$\sum_{\alpha,\beta} q_\alpha q_\beta S_{\alpha\beta}^*(\mathbf{q}, \omega) = \frac{\rho k_B T i \omega}{(1+b^*)(1+b)} \sum_\gamma \frac{\hat{q}_\gamma^2}{a_\gamma^* a_\gamma}. \quad (\text{D4})$$

-
- [1] Devonshire A F 1954 Theory of ferroelectrics *Adv. in Phys.* **3** 85-130
 - [2] Jona F and G. Shirane G 1962 *Ferroelectric crystals*, Pergamon press, Oxford
 - [3] Mitsui T, Nakamura E and Tokunaga M 1973 Critical phenomena in ferroelectric phase transitions I. Experimental observations and qualitative discussion *Ferroelectrics* **5** 185-196
 - [4] Landau L D and Lifshitz E M 1934 *Electrodynamics of Continuous Media* Pergamon, New York.
 - [5] Strukov B and Levanyuk A 1998 *Ferroelectric phenomena in crystals: Physical foundations* Springer, Berlin
 - [6] Tagantsev A K, Cross L E and Fousek J 2010 *Domains in Ferroic crystals and thin films* Springer
 - [7] Ghosez P and Junquera J 2022 Modeling of ferroelectric oxide perovskites: from first to second principles *Annu. Rev. Condens. Matter Phys.* **13** 325-364

- [8] Wen H, Liu J, Li J, Li B, Chen W and Zheng Y 2025 A review of progress in theoretical modeling of polarization dynamics in ferroelectric materials, *J. Phys.: Condens. Matter* **37** 173003
- [9] Samara G A 1971 Pressure and temperature dependence of the dielectric properties and phase transitions of the ferroelectric perovskites: PbTiO_3 and BaTiO_3 *Ferroelectrics* **2** 277-289
- [10] Clarke R and Benguigui L 1977 The tricritical point in BaTiO_3 *J. Phys. C: Solid State Phys.* **10** 1964-1973
- [11] Decker D L and Zhao Y X 1989 Dielectric and polarization measurements on BaTiO_3 at high pressures to the tricritical point *Phys. Rev. B* **39** 2432-2438
- [12] Mazur O, Tozaki K, Yoshimura Y and Stefanovich L 2022 Influence of pressure on the kinetics of ferroelectric phase transition in BaTiO_3 , *Physica A* **599** 127436
- [13] Ginzburg V L 1961 Some Remarks on Phase Transitions of the Second Kind and the Microscopic theory of Ferroelectric Materials *Soviet Phys. Solid State* **2** 1824-1834
- [14] Chandra P and Littlewood P B 2007 A Landau primer for ferroelectrics. In: *Physics of ferroelectrics. topics in applied physics*, **105** 69-116 Springer, Berlin, Heidelberg
- [15] Cao W and Cross L E 1991 Theory of tetragonal twin structures in ferroelectric perovskites with a first-order phase transition *Phys. Rev. B* **44** 5-12
- [16] Nambu S and Sagara A 1994 Domain formation anti elastic long-range interaction in ferroelectric perovskites *Phys. Rev. B* **50** 5838-5847
- [17] Hu H-L and Chen L Q 1998 Three-dimensional computer simulation of ferroelectric domain formation *J. Am. Ceram. Soc.* **81** 492-500
- [18] Onuki A 2002 *Phase Transition Dynamics* Cambridge University Press, Cambridge
- [19] Kretschmer J R and Binder K 1979 Surface effects on phase transitions in ferroelectrics and dipolar magnets *Phys. Rev. B* **20** 1065-1076
- [20] Brody E M and Cummins H Z 1968 Brillouin scattering study of the ferroelectric transition in KH_2PO_4 *Phys. Rev. Lett.* **21** 1263-1266
- [21] Garland C W and Novotny D B 1969 Ultrasonic velocity and attenuation in KH_2PO_4 *Phys. Rev.* **177** 971-975
- [22] Litovitz T A and Uehling E A 1970 Polarization relaxation and susceptibility in the ferroelectric transition region of KD_2PO_4 *Phys. Rev. B* **1** 3713-3724
- [23] Reese R L, Fritz J J and Cummins H Z 1973 Light scattering studies of the soft ferroelectric

- and acoustic modes of KD_2PO_4 *Phys. Rev. B* **7** 4165-4185
- [24] Landau L D and Khalatnikov I M 1954 On the anomalous absorption of sound near a second order phase transition point *Dokl. Akad. Nauk SSSR* **96** 469-472 Part of *Collected papers of L.D. Landau* 626-629
- [25] Krivoglaz M A 1963 Effect of long-range forces on fluctuations and the scattering of waves in crystals *Fiz. Tverd.* **5** 3437; *Sov. Phys.-Solid State* **5** 2526 (1964)
- [26] Geguzina S Ya and Krivoglaz M A 1967 Influence of long range dipole dipole forces on attenuation and velocity of ultrasound in ferroelectrics near second order transition point *Fiz. Tverd. Tela* **9** 3095; English transl *Soviet Phys.Solid State* **9** 2441 (1968)
- [27] Uchino K, Nnomura S, Cross L E, Newham R E and Jang Sei J 1981 Electrostrictive effect in perovskites and its transducer applications, *J.of Mater. Sci.* **16** 569-578
- [28] Yamada T 1972 Electromechanical properties of oxygen-octahedra ferroelectric crystals *J. Appl. Phys.* **41** 328-338
- [29] Uwe H and Sakudo T 1975 Electrostriction and stress-induced ferroelectricity in KTaO_3 *J. Phys. Soc. Jpn.* **38** 183-189
- [30] Bell A J 2001 Phenomenologically derived electric field-temperature phase diagrams and piezoelectric coefficients for single crystal barium titanate under fields along different axes *J. Appl. Phys.* **89** 3907-3914
- [31] Li Y L, Cross L E and Chen L Q 2005 A phenomenological thermodynamic potential for single crystals ? *J. Appl. Phys.* **98** 064101
- [32] Wang J J, Meng F Y, Ma X Q, M. Xu X and Chen L Q 2010Furthermore, i Lattice, elastic, polarization, and electrostrictive properties of BaTiO_3 from first-principles, *J. Appl. Phys.* **108** 034107
- [33] Hlinka J and Márton P 2006 Phenomenological model of a 90° domain wall in BaTiO_3 -type ferroelectrics *Phys. Rev. B* **74** 104104
- [34] Renoud R, Ragheb M, Borderon C, Gundel H W and Damamme G 2013 Free energy of BaTiO_3 single crystal, in *Applications of Ferroelectric and Workshop on the Piezoresponse Force Microscopy (ISAF/PFM)* Prague 34-37
- [35] Levanyuk A P 1965 Contribution to a phenomenological theory of sound absorption near second-order phase transition points *Sov. Phys. JETP* **22** 901-906 (1966): *J. Exptl. Theoret. Phys. (U.S.S.R.)* **49** 1304-1312 (1965)

- [36] Dvořák V 1971 A phenomenological theory of ultrasonic attenuation in ferroelectrics, *Czech. J. I 21* 836-845
- [37] Minaeva A, Levanyuk A P, Strukoy B A and Koptsik V A 1967 Absorption in of ultrasound during phase transitions in triglycine-type ferroelectrics *Fiz. Tverd. Tela* **9** 1220-1226 (1967); *Sov. Phys. Solid State* **9**, (1968) 950-954 (1968).
- [38] Minaeva K A, Strukov B A and Varnstorff K 1968 Anisotropy of sound absorption in triglycine sulfate (TGS) single crystals *Fiz. Tverd. Tela* **10** 2125-2128 (1968); *Sov. Phys. Solid State* **10** 1665-1667(1968)
- [39] O'brien E J and Litovitz T A 1964 Ultrasonic relaxation near the Curie temperature of ferroelectric triglycine sulfate *J. Appl. Phys.* **35** 180-186
- [40] Kashida S, Hatta I, Ikushima A and Yamada Y 1973 Ultrasonic velocities in BaTiO₃ *J. Phys. Soc. Jpn.* **34** 997-1001
- [41] Lee J W, Ko J -H, Roleder K and Rytz D 2019 Complete determination of elastic stiffness coefficients and local symmetry breaking in the paraelectric barium titanate *Appl. Phys. Lett.* **114** 072901
- [42] Yamada Y and Shirane G 1969 Lattice-dynamical study of the 110°K phase transition in STiO₃ *Phys. Rev. B* **177** 848-857
- [43] Yamada Y, Shirane G and Linz A 1969 Study of critical fluctuations in BaTiO₃ by neutron scattering *Phys. Rev. B* **177** 848-857
- [44] Paul G L, Cochran W, Buyers W J L and Cowley R A 1970 Ferroelectric transition in KD₂PO₄ *Phys. Rev. B* **2** 4603-4612
- [45] Riste T, Samuelsen E J, Otnes K and Feder J 1971 Critical behaviour of SrTiO₃ near the 105°K phase transition *Solid State Comu.* **9** 1455-1458
- [46] Shapiro S M, Axe J D, Shirane G and Riste T 1Furthermore, i72 Critical Neutr on Scattering in SrTiO₃ and KMnF₃ *Phys. Rev. B* **6** 4332-4341
- [47] Töppler J, Alefeld J B and Kollmar A 1975 Investigation of the central component of SrTiO₃ by neutron scattering with eV eV resolution Volume SI1A, number 5 *Phys. Lett.* **24** 297-298
- [48] Lyons K B and Fleury P A 1976 Dynamic central peaks in a crystalline solid: KTaO₃ *Phys. Rev. Lett.* **37** 161-164
- [49] Fleury P A and Lyons K B 1976 Central-peak dynamics at the ferroelectric transition in lead germanate *Phys. Rev B* **37** 1088-1091

- [50] Mermelstein M D and Cummins H Z 1977 Dynamic central peak in ferroelectric KH_2PO_4 *Phys. Rev. B* **16** 2177-2183
- [51] Sawafuji M, Tokunaga M and Tatsuzaki I 1979 Light scattering spectra depending on the direction of scattering wave vector in KD_2PO_4 . I Brillouin spectrum and broad central component *J. Phys. Soc. Jpn.* **47** 1860-1869
- [52] Luspin Y, Servoin J L and Gervais F 1980 Soft mode spectroscopy in barium titanate *J. Phys. C. Solid St. Phys.* **13** 3761-3773
- [53] Ko J -H, Kojima S, Koo T -Y, Jung J H, Won C J and Hur N J 2008 Elastic softening and central peaks in BaTiO_3 single crystals above the cubic-tetragonal phase-transition temperature *Appl. Phys. Lett.* **91** 102905
- [54] Jae-H. Ko J -H, T. H. Kim T H, K. Roleder K, D. Rytz D and S. Kojima S 2011 Precursor dynamics in the ferroelectric phase transition of barium titanate single crystals studied by Brillouin light scattering *Phys. Rev. B* **84** 094123
- [55] Yagi T, Tokunaga M and Tatsuzaki T 1976 Brillouin scattering studies of the uniaxial ferroelectric phase transition in TGS and TGSe *J. Phys. Soc. Jpn.* **40** 1659-1667
- [56] Miyakawa K and Yagi T 1980 A central peak in the light scattering spectra of the ferroelectric TGS *J. Phys. Soc. Jpn.* **49** 18
- [57] Tsujimi Y, Matsui T, Furuta H and Yagi T 1999 Physical origin of the dynamical central peak in ferroelectric triglycine sulfate *Phys. Rev. B* **59** 28-31
- [58] Halperin B I and Varma C M 1976 Defects as we find near structural phase transitions *Phys. Rev. B* **14** 4030
- [59] Cook H E 1977 Droplet model for central yphonon peaks *Phys. Rev. B* **15** 1477
- [60] Ginzburg V L, Levanyk A P and Sobyenin A A 1980 Light scattering near phase transition points in solids *Phys. Rep.* **57** 151-240
- [61] Burns G and Dacol F H 1982 Polarization in the cubic phase of BaTiO_3 *Solid State Commun.* **42** 9-12
- [62] Vacher R. and Boyer L 1972 Brillouin Scattering: A tool for the measurement of elastic and photoelastic Constants *Phys. Rev.* **6** 639-673
- [63] Cochran W 1969 Dynamical, scattering and dielectric properties of ferroelectric crystals *Adv. in Phys.* **18** 157-192
- [64] Stengel M, Spaldin N A and Vanderbilt D 2009 Electric displacement as the fundamental

- variable in electronic-structure calculations *Nature Phys.* **5** 304-308
- [65] Zhang C, Sayer T, Hutter J and Sprik M 2020 Modelling electrochemical systems with finite field molecular dynamics, *J. Phys. Energy*, **2** 032005
- [66] Dufils T, Sprik M and Salanne M 2021 Computational amperometry of nanoscale capacitors in molecular simulations *J. Phys. Chem. Lett.* **12** 4357-4361
- [67] Onuki A 2024 Ions and dipoles in electric field: nonlinear polarization and field-dependent chemical reaction *Eur. Phys. J. E* **47**:3
- [68] Onuki A 2025 Static and dynamic theory of polarization under internal and directing electric fields: Fixed-charge and fixed-potential conditions *J. Chem. Phys.* **162** 214105
- [69] Landau L D and Lifshitz E M 1986 *Theory of Elasticity* Pergamon Press
- [70] Fleming P D and Cohen C 1976 Hydrodynamics of solids *Phys. Rev. B* **13** 500-516
- [71] Mabillard J and Gaspard P 2021 Nonequilibrium statistical mechanics of crystals *J. Stat. Mech.* 063207
- [72] Mabillard J and Gaspard P 2024 Hydrodynamic correlation and spectral functions of perfect cubic crystals *J. Stat. Mech.* 033204
- [73] Schlosser R and Drougard M E 1961 Surface layers on barium titanate single crystals above the Curie point *J. Appl. Phys.* **32** 1227-1231
- [74] Sekido T and Mitsui T 1967 Dielectric constant of triglycine sulfate at the Curie point *J. Phys. Chem. Solids* **28** 967-970
- [75] Chincholtur V S and Unruh H -G 1968 Surface layers of triglycine sulfate single crystals *Phys. Stat. Sol.* **29** 669-673
- [76] Mansingh A and Prasad S R J E 1976 Dielectric behavior of ferroelectric triglycine sulphate near the transition temperature *J. Phys. D: Appl. Phys.* **9** 1379-1386
- [77] Chang L -W, Alexe M, Scott J F and Gregg J M 2009 Settling the "dead layer" debate in nanoscale capacitors *Adv. Mater.* **21** 4911-4914
- [78] Stengel M, Vanderbilt D and Spaldin N A 2009 Enhancement of ferroelectricity at metal ? oxide interfaces *Nature Mater.* **8** 392-397
- [79] Majdoub M S, Maranganti R and P. Sharma P 2009 Understanding the origins of the intrinsic dead layer effect in nanocapacitors *Phys. Rev. B* **79** 115412
- [80] Tagantsev K and Gerra G 2006 Interface-induced phenomena in polarization response of ferroelectric thin films *J. of App. Phits.* **100** 051607

- [81] Hamann C H, Hamnett A and Vielstich W 2007 *Electrochemistry* Wiley VCH
- [82] Takae K and Onuki A 2015 Fluctuations of local electric field and dipole moments in water between metal walls *J. Chem. Phys.* **143** 154503
- [83] Olivieri J -F, Hynes J T and Laage D 2021 Confined water's dielectric constant reduction is due to the surrounding low dielectric media and not to interfacial molecular ordering *J. Phys. Chem. Lett.* **12** 4319-4326
- [84] Cox S J and Geissler P L 2022 Dielectric response of thin water films: A thermodynamic perspective *Chem. Sci.* **13** 9102-9111
- [85] Fumagalli L, Esfandiar A, Fabregas R, Hu1 S, Ares1 P, Janardanan A, Yang Q, Radha B, Taniguchi, Watanabe K, Gomila G, Novoselov K S and Geim A K 2018 Anomalously low dielectric constant of confined water *Science* **360** 1339-1342
- [86] Amit D 1974 The Ginzburg criterion-rationalized *J. Phys. C: Solid State Phys.* **7** 3369-3377
- [87] Fedorov F I and Fedorov A F 1991 On the structure of the Green-Christoffel tensor *J. Phys. A: Math. Gen.* **24** 71-78
- [88] Aharony A and Fisher M E 1973 Critical behavior of magnets with dipolar interactions. I. Renormarization group near four dimensions *Phys. Rev.B* **8** 3323-3341
- [89] Grabovsky S V, Shnaidshtein I V, Takesada M, Onodera A and Strukov B A 2013 Calorimetric study of ferroelectric BaTiO₃ in cubic phase *J. of Adv. Dielectrics* **3** 1350032
- [90] Hatta I and Ikushima A J 1981 Studies on phase transitions by AC calorimetry *Jpn. J. Appl. Phys.* **20** 1995-2011
- [91] Halperin B I, Hohenberg P C and Ma S K 1974 Renormalization-group methods for critical dynamics: I. Recursion relations and effects of energy conservation *Phys, Rev. B* **10** 139-153
- [92] Onuki A 1989 Ginzburg-Landau approach to elastic effects in phase separation in solids *J. Phys. Soc. Jpn.* **58** 3065-3068
- [93] Kadanoff L P and Martin P C 1963 Hydrodynamic Equations and Correlation Functions *Ann. Phys.* **24** 419-469
- [94] Zykova V A, Karpegina Y A, Malinovsky V K and N. V. Surovtsev N V 2017 Temperature dependence of the Landau-Placzek ratio in liquid water *Phys. Rev. E* **96** 042608
- [95] Nishimori H and Onuki A 1990 Pattern formation in phase-separating alloys with cubic symmetry *Phys. Rev.B* **42** 980-983
- [96] Hubbard J and Onsager L 1977 Dielectric dispersion and dielectric friction in electrolyte

- solutions *J. Chem. Phys.* **67** 4850-4856
- [97] Ladanyi B M and Skaf M S 1996 Wave vector-dependent dielectric relaxation of methanol-water mixtures *J. Phys. Chem.* **100** 1368-1380
- [98] Hill R M and Ichiki S K 1963 High-Frequency Behavior of Hydrogen-Bonded Ferroelectrics: Triglycine Sulphate and KD_2PO_4 *Phys. Rev.* **132** 1603-1608
- [99] Hatta I 1968 Experimental study on dielectric relaxation in NaNO_3 *J. Phys. Soc. Jpn.* **24** 1043-1053
- [100] Vogt H, Sanjurjo J A and Rossbroich G 1982 Soft-mode spectroscopy in cubic BaTiQ_3 by hyper-Raman scattering *Phys. Rev. B*, **26** 5904
- [101] Ponomareva I, Bellaiche L, Ostapchuk T, Hlinka J and Petzelt J 2008 Terahertz dielectric response of cubic BaTiO_3 *Phys. Rev. B* **77** 012102
- [102] Zaccone A 2023 General theory of the viscosity of liquids and solids from nonaffine particle motions *Phys. Rev. E* **108** 044101
- [103] Mori H 1965 Transport, collective motion, and Brownian motion *Progr. Theor. Phys.* **33** 423-455
- [104] Kawasaki K 1970 Sound attenuation and dispersion near the liquid-gas critical point *Phys. Rev.* **1** 1750-1757
- [105] Kubo R 1957 Statistical mechanical theory of irreversible processes. I, *J. Phys. Soc. Jpn.* **12** 570-586 .
- [106] Kawasaki K 1969 A note on the ultrasonic attenuation near the magnetic critical point *Phys. Lett.* **29A** 406-407
- [107] Laramore G E and Kadanoff L P 1969 Anomalous ultrasonic attenuation above the magnetic critical point *Phys. Rev. E* **187** 619-628
- [108] Onuki A 1997 Dynamic equation and bulk viscosity near the gas-liquid critical point *Phys. Rev. E* **55** 403-420